

Neural Correlates of Eye Contact and Social Function in Autism Spectrum Disorder

1 ***Joy Hirsch^{1, 2, 4, 5, 6, 7}, Xian Zhang¹, J. Adam Noah¹, Swethasri Dravida^{1, 2}, Adam Naples³,**
2 **Mark Tiede^{1, 7}, Julie M. Wolf³, and *James C. McPartland³**

3 ¹Brain Function Laboratory, Department of Psychiatry, Yale School of Medicine, 300 George St.,
4 Suite 902, New Haven, CT, USA

5 ²Interdepartmental Neuroscience Program, Yale School of Medicine, New Haven, CT, 06511, USA

6 ³Yale Child Study Center, Nieson Irving Harris Building, 230 South Frontage Road, Floor G, Suite
7 100A, New Haven, CT, 06519, USA

8 ⁴Department of Neuroscience, Yale School of Medicine, New Haven, CT, 06511, USA

9 ⁵Department of Comparative Medicine, Yale School of Medicine, New Haven, CT, 06511, USA

10 ⁶Department of Medical Physics and Biomedical Engineering, University College London, London,
11 WC1E 6BT, UK

12 ⁷Haskins Laboratories, 300 George St., Suite 900, New Haven, CT, 06511, USA

13

14 ***Two Corresponding authors:**

James C. McPartland, PhD
Yale Child Study Center
Nieson Irving Harris Building
230 South Frontage Road
Floor G, Suite 100A
New Haven, CT, 06519
james.mcpartland@yale.edu
203.785.7179

Joy Hirsch, PhD
Yale School of Medicine
Department of Psychiatry
Brain Function Laboratory
300 George St, Suite 902
New Haven, CT, 06511

15 **Keywords:** autism spectrum disorder (ASD), live eye-to-eye contact, interactive face
16 processing, dorsal stream, functional near-infrared spectroscopy (fNIRS), hyperscanning,
17 social symptomatology, visual sensing

18 **Abstract**

19 Reluctance to make eye contact during natural interactions is a central diagnostic criterion
20 for autism spectrum disorder (ASD). However, the underlying neural correlates for natural
21 eye contacts in ASD are unknown, and diagnostic biomarkers are active areas of
22 investigation. Here, neuroimaging, eye-tracking, and pupillometry data were acquired
23 simultaneously using two-person functional near-infrared spectroscopy (fNIRS) during live
24 eye-to-eye contact and eye-gaze at a video face in typically developed (TD) and ASD
25 participants to identify the neural correlates of live eye-to-eye contact in both groups. Direct
26 comparisons between ASD and TD participants showed decreased right dorsal parietal
27 activity and increased right ventral temporal-parietal activity for ASD relative to TD during
28 live eye-to-eye contact ($p \leq 0.05$, FDR-corrected) consistent with the hypothesis of alternative
29 neural systems for live eye contact. The additional hypothesis that hypoactivity of the right
30 dorsal-parietal regions during eye contact is associated with social performance in ASD was
31 supported by the correlation of right dorsal parietal activity with individual measures of social
32 function: ADOS-2, Autism Diagnostic Observation Schedule, 2nd Edition ($r = -0.69$); and
33 SRS-2, Social Responsiveness Scale, Second Edition ($r = -0.58$). That is, as social ability
34 decreased, the neural responses in the right dorsal parietal region to real eye-contact also
35 decreased consistent with a neural correlate for social characteristics in ASD.

36

37

38 Introduction

39 Eye contact with another human is an impactful and fundamental component of in-
40 person social behavior. Intermittent eye-to-eye fixations are widely thought of as particularly
41 potent stimuli. For example, proverbial claims that “the eyes are the window to the soul” are
42 taken as self-evident, and eye-to-eye contact is attributed with literary properties such as
43 the “spark” that ignites a “social connection” and the sharing of information. Wisdom
44 regarding the social significance of eye gaze is long-standing in classical literature and may
45 have its source in a quote from Marcus Tullius Cicero’s *Orator*: “*Ut imago est animi voltus*
46 *sic indices oculi*” translated as, “For as the face is the image of the soul, so are the eyes its
47 interpreters” (1). Although there are cultural variations related to the interpretation of
48 interpersonal eye gaze (2-5), eye contacts universally signal social cues such as levels of
49 engagement, emotional status, intention, judgment, and an array of nuanced exchanges of
50 social information including an invitation for interaction. Direct eye contact with another
51 person is conventionally taken as a significant interaction, regardless of the cultural norms.
52 Given the salience of real face-to-face and dynamic eye-to-eye interactions, the
53 development of two-person methodologies and a theoretical framework for understanding
54 the neural biology of live face-to-face related social cues is a high priority.

55 Autism spectrum disorder (ASD) is a complex neurodevelopmental condition
56 including distinct behavioral, communicative, and social responses such as reluctance to
57 make eye contact during natural social interactions (6). The underlying neurobiology of ASD
58 is typically investigated by single non-interactive participants and, therefore, the biological
59 underpinnings of observed behavioral differences during live and interactive social
60 processes are not well understood. The single participant focus of conventional
61 neuroimaging is a contributing factor to this knowledge gap, as the neural systems that
62 underlie social differences in ASD cannot be directly investigated in passive stimulus-

63 response paradigms. Nonetheless, single participant stimulation paradigms have
64 contributed the foundation for the basic neuroscience of social ability in ASD.

65 For example, in the case of visual sensing and low-level visual processes, variations
66 in patterns of eye-gaze are well documented in ASD (7-15). Reduced responses to
67 emotional cues conveyed by simulated facial dynamics (16) and reduced production of facial
68 expressions that signal emotional content (17-20) have also been reported. Reduced
69 occipital pole responses to pictured eyes for ASD participants observed by fMRI suggest
70 atypical early visual processing (21). Eye gaze at pictured eyes with emotional content has
71 been associated with abnormally high activation in subcortical systems including superior
72 colliculus, pulvinar nucleus of the thalamus, and the amygdala. Elevated amygdala
73 responses to neutral faces have also been associated with eye gaze suggestive of increased
74 arousal for face stimuli (22).

75 Electroencephalography (EEG) findings in ASD show increased latency of event-
76 related potentials (ERPs) to pictured eye stimuli relative to typically developed (TD)
77 participants (23, 24). This latency has been shown to be related to gaze directed at the eyes
78 of a pictured face in TD individuals (Parker et al., 2021). Atypical and reduced responses to
79 simulated faces and robots have also been shown using fNIRS in support of the hypothesis
80 of alternative neural pathways for face processing (25).

81 Temporal cortex is activated specifically during viewing of eye movements in the TD
82 population as shown by fMRI and electrophysiology and confirmed by primate
83 neurophysiology (26-29). In contrast, in ASD, hypoactivation of superior temporal sulcus and
84 face-related dorsal areas consisting of the somatosensory and premotor cortex previously
85 associated with face processing have also been reported (30). Atypical brain activation
86 patterns during face-to-face joint attention in adults with ASD revealed reduced signal
87 differentiation between joint attention and control conditions within the superior temporal

88 sulcus and dorsal medial prefrontal cortex (31). Hypoactive high-level cognitive and
89 language systems have also been reported (32, 33). These prior findings of atypical early
90 and higher-order perceptual, cognitive, and language processing are consistent with the
91 overarching hypothesis of impacted social-communicative systems related to face and eye-
92 processing in ASD (34).

93 In natural real-life situations, humans typically perceive complex facial information
94 conveyed by facial expressions within very brief exposures including subliminal
95 presentations of fearful faces (35). Dynamic and reciprocal face interactions are primary
96 sources of social information and streaming of cues extracted from faces guide real live
97 perceptions and behaviors. However, self-declared autistic adolescents and adults have
98 reported struggling with flexibly and strategically extracting information from the face using
99 eye gaze during face-to-face interactions (36). The importance of investigating real-life facial
100 interactions in ASD has been recognized by recent calls for “second-person neuroscience”
101 (37-39). A theoretical context for this notion in clinical applications has been proposed as
102 “second person neuropsychiatry” (Schilbach, 2016) aimed at the development of
103 quantitative assessments of dyadic social interactions referred to “interaction-based
104 phenotyping” (Schilbach, 2019). However, the paucity of neuroimaging techniques to
105 acquire dyadic information on dynamic face processing during real social interactions has
106 challenged advances in the development of these methods and in understanding the
107 underlying neurobiology of these processes (40, 41) and their variations in ASD.

108 In response to this knowledge gap, recent developments in functional near-infrared
109 spectroscopy (fNIRS) have applied hyperscanning (simultaneous brain scanning of two
110 individuals during live interactions) to pave the way for much-needed studies of live
111 interactions between individuals and investigations of neural substrates associated with
112 atypical social interactions. Technical advances in fNIRS (42, 43) and the immediate need

113 to understand the biological components of live and interactive human social behaviors have
114 supported the emergence of neuroimaging technology to investigate dynamic face-to-face
115 and eye contact behaviors in ASD.

116 The current investigation aims to identify neural systems responsive to *in vivo* eye
117 contact in both ASD and TD and to examine their relationship to social performance. The
118 overarching hypothesis is that interactive face processing, with eye contact being a central
119 component, engages complex neural encoding of high-level demands for rapid interpretation
120 of subtle eye movements and facial cues that convey social meaning. These cues are not
121 included in non-interactive and conventional simulated face stimuli. Thus, it is expected that
122 neural processing of interactive faces in ASD and TD groups will include social systems
123 (44); interactive face processing systems (45-47); and motion-sensitive systems (48)
124 hypothesized to be differentiated between TD and ASD groups. Here we test the specific
125 hypothesis that individual differences in social function in ASD are predicted by neural
126 responses associated with live eye-to-eye contact.

127 TD and ASD adults were compared during real gaze at the eyes of a same-sex lab
128 partner and gaze at a comparable dynamic face video (instructions were to gaze at the eyes
129 under both conditions). In the real-person interaction condition (Real Eye), partners viewed
130 each other's faces directly while sitting across a table from one other. Findings were
131 compared with a condition in which participants and their lab partners both viewed the eyes
132 of a size-matched face displayed on a video monitor (Video Eye). The contrast between
133 these two conditions and direct comparisons between ASD and TD groups tested the
134 hypothesis that neural processes responsive to real eye-to-eye contact are altered in ASD
135 relative to TD. Eye tracking and pupillometry during these conditions were used to test the
136 related hypothesis that gaze characteristics (visual sensing) and an autonomic indicator of
137 arousal (pupil size variation) also varied during face processing between TD and ASD. The

138 social performance for all ASD participants was assessed by clinical interview, including
139 administration of the Autism Diagnostic Observation Schedule (2nd Edition, ADOS-2) (49).
140 Self-report measures were given to both ASD and TD participants, including the Social
141 Responsiveness Scale (Second Edition, SRS-2) (50). A goal of this investigation was to
142 determine how these social metrics of behavioral function related to eye contact were linked
143 to the underlying neurophysiology.

144 **Methods and Materials**

145 **Participants.** Participants included 17 healthy Autism Spectrum Disorder (ASD) adults (3
146 female; mean age 25 ± 4.9 years; 12 right-handed, 3 left-handed, and 2 ambidextrous (51))
147 whose diagnoses were verified by gold standard, research-reliable clinician assessments,
148 including the Autism Diagnostic Observation Schedule, 2nd Edition (ADOS-2 (49)) (Table
149 S1), and expert clinical judgment using DSM-5 criteria (6); and 19 healthy, typically-
150 developed (TD) adults (mean age 26 ± 5.8 years; 18 right-handed and 1 ambidextrous) (Table
151 S2). Participants were recruited from ongoing research in the McPartland Lab, the Yale
152 Developmental Disabilities Clinic, and the broader community through flyers and social
153 media announcements. Inclusion criteria included age 18-45 years, $IQ\geq 70$, and English
154 speaking. Exclusion criteria included diagnosis of bipolar disorder, personality disorder, or
155 schizophrenia spectrum disorder; anti-epileptic, barbiturate, or benzodiazepine medication
156 use; history of seizures, brain damage, or recent serious concussion; alcohol use within 24
157 hours; recreational drug use within 48 hours; chronic drug abuse; medication changes within
158 two weeks; sensory impairment or tic disorder that would interfere with fNIRS recording;
159 history of electroconvulsive therapy; or genetic or medical condition etiologically related to
160 ASD. Additional exclusionary criteria for TD participants included self-report of any
161 psychiatric diagnosis or learning/intellectual disability; psychotropic medication; or a first-

162 degree relative with ASD. All participants provided written and verbal informed consent in
163 accordance with guidelines and regulations approved by the Yale University Human
164 Investigation Committee (HIC #1512016895) and were reimbursed for their participation.
165 Assessment of the ASD participants' capacity to give informed consent was provided by a
166 consensus of trained professional staff who monitored the process and confirmed verbal
167 and non-verbal responses. In order to assure that participants were comfortable during the
168 experimental procedure, ASD participants were accompanied at all times by a member of
169 the clinical team, who continuously evaluated their sustained consent to participate.

170 All participants were characterized by gender, age, full-scale IQ (FSIQ-4 as estimated
171 by the Wechsler Abbreviated Scale of Intelligence, 2nd Edition (WASI-II; (52), and self-
172 reported clinical characteristics on several questionnaires, including the Autism-Spectrum
173 Quotient (AQ; (53); Broad Autism Phenotype Questionnaire (BAPQ; (54); Social
174 Responsiveness Scale, Second Edition (SRS-2; (50); Beck Anxiety Inventory (BAI; (55);
175 State-Trait Anxiety Inventory (STAI; (56); and the Liebowitz Social Anxiety Scale (LSAS;
176 (57)). See Tables S3 and S4 for detailed demographic and statistical comparisons between
177 the two groups. Group comparisons of clinical assessments indicated expected differences
178 on the AQ ($p \leq 0.01$); BAPQ ($p \leq 0.01$); SRS-2 ($p \leq 0.01$); and BAI scales ($p \leq 0.05$), and failed to
179 provide evidence for differences on the WASI-II, STAI, and LSAS between the groups.
180 Assessment and diagnostic tests were performed in clinical facilities at the Yale Child Study
181 Center.

182 Participants were escorted from the clinical environment to the research environment
183 for fNIRS / eye tracking experiments. An investigator was present during the data acquisition
184 and monitored signs of discomfort during the experiment. All participants were paired with a
185 same-gender TD lab partner. One male and one female, both in their 20's, served as lab
186 partners throughout the entire study. Lab partners were not informed of the participant's

187 group membership before the experiment.

188 Determination of a sample size sufficient for a conventional power of 0.80 was based
189 on contrasts (Real face > Video Face) reported in a previous study using similar two-person
190 techniques with a lab partner (47). Using the pwr package of R statistical computing software
191 (58), a significance level of $p < 0.05$ is achieved with 16 participant/lab partner dyads.
192 Sample sizes of 34 (17 ASD dyads) and 38 (19 TD dyads) ensure adequate effect sizes for
193 these paired experiments. Although sufficient for the planned and reported analyses, a larger
194 sample size would ordinarily be preferred. However, COVID related circumstances have
195 prevented further acquisitions.

196 ***Experimental Procedures and Paradigm.*** Dyads (participant and a gender-matched lab
197 partner) were seated 140 cm across a table from each other and were fit with an extended
198 head-coverage fNIRS cap. Each participant was either instructed to look straight ahead
199 either at their partner or at a monitor with a video face adjusted in size to subtend the same
200 visual angles as the real face (Fig 1A and B). In the live (Real Eye) task, dyads were
201 instructed to gaze at each other's eyes during cued 3-second epochs (1A), and in the video
202 (Video Eye) task, dyads were instructed to gaze at the eyes of the face as it appeared in the
203 dynamic video (1B). The illustrative red box enclosing the eyes of the participants in Fig 1
204 subtended $3.3 \times 1.5^\circ$ of visual angle and defined the location of the "eye box," a region
205 designated as the eye contact zone for each participant. In both tasks, dyads alternated their
206 gaze between the eyes of their (real or video) partner and two small light-emitting diodes
207 (LEDs) located 10° to the left and 10° to the right of their partner's face (Figs 1C and D).
208 The video was a recorded version of a same-gender participant performing the same task
209 while wearing the same optode cap as live participants.

210 **Figure 1. Eye gaze tasks. A.** Gaze at partner's eyes: Real Eye condition. Partners viewed each
211 other at an eye-to-eye distance of 140 cm. The eye regions subtended by both the real eyes and the

212 video eyes were 3.3×1.5 degrees of visual angle (red boxes). Small green LED indicator lights
213 located to either side of their partner indicated rest and diverted gaze targets. **B.** Gaze at eyes in
214 video: Video Eye condition. Two 24-inch 16x9 monitors were placed between the participants and a
215 size-calibrated, pre-recorded dynamic video of a face was presented in the same field-of-view as the
216 live interaction. **C.** Diagram of the Real Eye condition, with participant and lab partner sitting 140 cm
217 apart from each other and LED indicator lights placed 10 degrees to the left and right of the Eye. **D.**
218 Diagram of the Video Eye condition, with monitors arranged between partners. The face and LED
219 sizes and positions were calibrated to subtend the same visual angles in both conditions.
220

221 The order of runs was randomly sequenced between viewing a real partner directly
222 or viewing the visual-angle corrected video partner on a 24-inch 16x9 computer monitor
223 placed back-to-back between participants, including a partition to assure that dyads could
224 not see their real partner during video conditions. The face and distance of the video stimuli
225 were calibrated to subtend identical degrees of visual angle in the field of view of the
226 participants and the timing and range of motion of eye movements between partners were
227 the same in both tasks. The time-series and experimental details were similar to prior studies
228 (45, 47) and are included here to provide a self-contained report.

229 At the start of each task, an auditory cue prompted participants to gaze at the eyes
230 of their real or recorded partner. Subsequent auditory tones alternately cued eye gaze
231 between eyes or LED according to the protocol time series. The 15-second active task
232 period alternated with a 15 s rest/baseline period. The task period consisted of three 6-
233 second cycles in which gaze alternated on the partner for 3 s and then on a lighted LED to
234 either the right or left (alternating) of the participant for 3 s for each of three events. The time
235 series was performed in the same way for all runs. The order of runs was counterbalanced
236 across pairs of participants. During the 15 s rest/baseline period, participants focused on the
237 lighted LED, as in the case of the 3 s periods that separated the eye contact and gaze events.
238 The 15 s activity epoch with alternating eye contact events was processed as a single block.

239 The experimental paradigm (Fig 2A) employed a classic hemodynamic time series

240 with 15 s of task alternating with 15 s of rest. Run length was 3 m and included six task-rest
241 cycles. Due to the social discomfort associated with prolonged mutual gaze at another's
242 eyes, the task epochs were subdivided into events (epochs) that alternated between three
243 3-second "eye-on" and 3-second "eye-off" cycles (see Fig 2A). During the "eye-on" epoch,
244 dyads were instructed to gaze at the eyes of their (real or video) partner, making eye contact
245 as often as possible in natural intervals. An auditory tone signaled the transition between
246 eye-on and eye-off events indicating when participants were instructed to divert their gaze
247 to the LED targets 10° to the right or left.

Figure 2. A. Time course. The duration of the run was three minutes and each run was repeated twice for both the Real Eye and Video Eye conditions. Each run included six alternating 15-second task and rest periods. In task periods (blue bars), participants alternated their gaze in three-second epochs between the eyes and the left or right lighted LED (See Fig 1, C and D). During the 15-second rest period, participants looked only at the lighted LED. The task is similar to those used in previous experiments (Hirsch et al., 2017; Noah et al., 2020). **B. Eye tracking traces of eye-to-eye contact.** Red traces represent eye movements from an ASD participant; blue traces represent the eye movements of a lab partner. The eye tracking data acquired on the Tobii system provides a frame-by-frame (8 ms) binary value that indicates whether or not eye gaze was directed within the eye-box of the partner. The blue dashed line (top) represents the duration of eye gaze (number of frames) that the lab partner's gaze was within the eye-box of the participant. Similarly, the red dashed line (bottom) represents the duration of gaze (number of frames) that the participant's eye gaze was in the eye-box of the lab partner. The green dashed line (middle) represents the length of time (number of frames) that the eyes of both partners were simultaneously focused within each other's eye-boxes for a minimum of 83 ms. This is taken as a measure of eye-to-eye contact between the participant and the lab partner. **C, D. Gaze performance, Real Eye condition.** Eye contact epochs (3 s) are indicated as E; Diverted gaze epochs (3 s) are indicated as D; and Rest periods (15 s) are indicated as R. The color bar (top) indicates the percent of time eye gaze was within the eye box of the partner. **C.** Example eye tracking report for one TD participant and lab partner pair. **D.** Example eye tracking report for one ASD participant and the lab partner pair. Similar computations were performed for all participants when eye tracking data were acquired.

248

249 **Eye Tracking.** Two Tobii Pro x3-120 eye trackers (Tobii Pro, Stockholm, Sweden), one per
250 participant, were used to acquire simultaneous eye tracking data at a sampling rate of 120
251 Hz. Eye trackers were mounted on the table facing each participant. Prior to the start of the
252 experiment, a three-point calibration method was used to calibrate the eye tracker on each
253 participant. The partner was instructed to stay still and look straight ahead while the

254 participant was told to look first at the partner's right eye, then left eye, then the tip of the
255 chin. The same calibration procedure for video interactions was performed before recording
256 on a still image presented on the monitor 70 cm in front of the participants. Similar live
257 calibration procedures have been used successfully in prior investigations of in-person
258 social attention (59, 60). As instructed for the eye movement task, participants alternated
259 their gaze between $\approx 0^\circ$ and 10° of deflection. Participants fixated on the eyes of the video
260 (Video Eye condition) or the eyes of the lab partner (Real Eye condition) $\pm 10^\circ$ deflections to
261 either the left or right. The eye contact portions of the task were 3 s in length, with six per
262 trial, for 18 s of expected eye contact over the trial duration (Fig 2B).

263 Eye tracking provided a measure of compliance with task instructions to fixate on the
264 eye as illustrated in Fig 2B for a lab partner (blue trace) and an ASD participant (red trace).
265 The x-axis represents the run time series (180 s), and the y-axis represents the gaze angle,
266 where 0 represents eye-to-eye contact and $\pm 10^\circ$ indicate left and right deflections,
267 respectively. The moments of dyadic eye contact (gaze is within the eye box of their partner)
268 are indicated by the green line. The time series of Fig 2A and 2B are synchronized for
269 illustrative purposes. The blue and red dashed lines above and below the eye position trace
270 indicate the times of gaze locations that are within the eye box of the partner for the lab
271 partner and the ASD participant respectively. An "eye box hit" is defined when the gazes of
272 both partners are within the designated eye box of the other for a minimum of 83 ms, i.e.,
273 10 frames (61). The green lines in the figure indicate these 10-frame time points where the
274 gaze of both partners was in the eye box of the other. The eye contact performance is
275 illustrated for a typical participant in Fig 2C and an ASD participant in Fig 2D by the color of
276 the event bar where the percentage of time in the eye box of the lab partner is represented
277 by the color bar for the entire run time (180 s). Examples of average gaze positions are

278 shown for 5 typical participants in Fig 3A to illustrate the gaze and eye box confirmation.

279

Figure 3. A. Examples of average participant eye gaze positions when viewing the face of the lab partner. The red box illustrates the target “eye box” and the color gradient from red to green indicates percent of “target hits” in the eye box for an entire run. **B.** fNIRS channel layout. Right and left hemispheres of a single rendered brain illustrate median locations (blue dots) for 58 channels per participant. Montreal Neurological Institute (MNI) coordinates were determined for each channel by digitizing emitter and detector locations in relation to anterior, posterior, dorsal, and lateral fiducial markers based on the standard 10-20 system.

280 **Functional NIRS Signal Acquisition and Channel Localization.** Functional NIRS signal
281 acquisition, optode localization, and signal processing, including global mean removal, were
282 similar to methods described previously (62-68) and are briefly summarized below.
283 Hemodynamic signals were acquired using 3 wavelengths of light, and an 80-fiber
284 multichannel, continuous-wave fNIRS system (LABNIRS, Shimadzu Corp., Kyoto, Japan).
285 Each participant was fitted with an optode cap with predefined channel distances. Three
286 sizes of caps were used based on the circumference of the heads of participants (60 cm,
287 56.5 cm, or 54.5 cm). Optode distances of 3 cm were designed for the 60 cm cap but were
288 scaled equally to smaller caps. A lighted fiber-optic probe (Daiso, Hiroshima, Japan) was
289 used to remove all hair from the optode channel before optode placement.

290 Optodes consisting of 40 emitters and 40 detectors were arranged in a custom matrix,
291 providing a total of 54 acquisition channels per participant. The specific layout with the
292 coverage of the optode channels is shown in Fig 3B. For consistency, placement of the most
293 anterior channel of the optode holder cap was centered 1 cm above nasion. To assure
294 acceptable signal-to-noise ratios, resistance was measured for each channel prior to
295 recording, and adjustments were made for each channel until all recording optodes were
296 calibrated and able to sense known quantities of light from each laser wavelength (63, 69,
297 70). Anatomical locations of optodes in relation to standard head landmarks were

298 determined for each participant using a Patriot 3D Digitizer (Polhemus, Colchester, VT) (71-
299 75). Montreal Neurological Institute (MNI) coordinates (76) for each channel were obtained
300 using NIRS-SPM software (77) with WFU PickAtlas (78, 79).

301 **Analysis of eye-to-eye contact, dwell time, and pupillary responses.** Eye tracking
302 information including pupil size was exported from the Tobii system to the data processing
303 pipeline and custom scripts in MATLAB where it was used to calculate the mutual eye
304 contact events, accuracy, latency to targets, and pupil diameters. Eye-tracking data were
305 not usable on 5 out of 17 ASD participants and 4 out of 19 TD participants due to either
306 calibration or equipment problems (right columns of Tables S1 and S2 summarize the eye
307 tracking acquisitions). Tobii Pro Lab software (Tobii Pro, Stockholm, Sweden) was used to
308 create areas of interest for subsequent eye tracking analyses run in MATLAB 2014a
309 (Mathworks, Natick, MA). The eye box was identified manually for each run and each
310 participant for both live and video sequences. For the measures of gaze duration and
311 variability, the horizontal components of gaze trajectories were gated by the eye-to-eye
312 portions of each trial, retaining only samples that were within the eye box range.

313 This analysis used the zero angle (eye contact) intervals to characterize participant
314 eye contact behavior. The eye tracking source was the horizontal component of post-
315 processed trajectories converted to units of arc length (tenths of a degree). There were 1350
316 observations of 27 participants (15 TD, 12 ASD). To avoid possible inclusion of the large
317 movements into and out of the valid range, the first and last 200 ms of each 3 s eye contact
318 interval were excluded. Three measures were obtained from each interval: Dwell Time, the
319 number of valid retained samples per interval normalized by sampling rate (seconds); Gaze
320 Variability, the standard deviation of the samples centered over each interval, normalized by
321 the number of retained samples (Figs 4A and B); and pupil diameter (mm) Figs 4C and D.
322 In the case of the gaze position data (Figs 4A and B) linear mixed-effect models were used

323 to assess the fixed effects of group (TD, ASD) and condition (Video Eye, Real Eye), with
324 random intercepts by participant. Pupil sizes for left and right eyes (Figs 4C and D) were
325 sampled at 40 Hz using the Tobii eye tracking system. All analyses used average pupil sizes
326 across both eyes. To match the temporal resolution of the gaze position data, the pupil
327 diameter data were interpolated to a sample rate of 120 Hz.

328 **fNIRS Signal Processing.** Raw optical density variations were acquired at three
329 wavelengths of light (780 nm, 805 nm, 830 nm), which were translated into relative
330 chromophore concentrations using a Beer-Lambert equation (80-82). Signals were recorded
331 at 30 Hz. Baseline drift was removed using wavelet detrending provided in NIRS-SPM (77).
332 In accordance with recommendations for best practices using fNIRS data (83), global
333 components attributable to blood pressure and other systemic effects (84) were removed
334 using a principal component analysis (PCA) spatial global mean filter (62, 64, 85) prior to
335 general linear model (GLM) analysis. All analyses are reported using the combined OxyHb
336 and deOxyHb signals. The deOxyHb signal is inverted so that a positive result corresponds
337 to increases in brain activity, similar to the OxyHb signal. The combined signal averages are
338 taken as the input to the second level (group) analysis (86). Comparisons between
339 conditions were based on GLM procedures using the NIRS-SPM software package. Event
340 epochs within the time series were convolved with the hemodynamic response function
341 provided from SPM8 (87) and were fit to the signals, providing individual “beta values” for
342 each participant across conditions. Group results based on these beta values were rendered
343 on a standard MNI brain template (TD-ICBM152 T1 MRI template (Mazziota et al., 2001) in
344 SP8 using NIRS-SPM software (77) with WFU PickAtlas (78, 79).

345 **Code Accessibility.** Custom code will be provided upon request at fmri.org.

346 **Results**

347 **Behavioral**

348 **Eye-to-eye contact.** Even though eye-to-eye contact is often reduced in individuals with
349 ASD, in this investigation, we asked our participants to look directly at the face of the lab
350 partner and to make eye-to-eye contacts during the cued 3-second periods. The recorded
351 measures of gaze time in the “eye box” did not differ systematically between TD and ASD
352 participants for either the Real Eye or Video Eye conditions (see Supplementary S1 and S2
353 Figs), confirming compliance with this task: a t-test of median eye box dwell time
354 percentages failed to provide evidence for differences between groups (see Supplementary
355 Table S5). This approach supports the assumption that both TD and ASD participants
356 performed the same task, i.e., eye-to-eye contact during the 3 s epochs. Gaze dwell time
357 assessed using a linear mixed effects model with fixed effects of Group and Condition and
358 random intercepts by participant showed no group difference or interaction, but dwell time
359 for both TD and ASD groups was significantly longer in the Real Eye condition ($t=10.88$,
360 $p\leq 0.001$). See Fig 4A. However, gaze variability (assessed as the standard deviation of the
361 horizontal component of eye trajectory during the eye contact intervals normalized by their
362 duration) was greater for the ASD than the TD group for both conditions, see Fig 4B,
363 consistent with altered visual sensing mechanisms in eye-movement patterns in ASD while
364 viewing the face and eye stimuli in either condition ($t=2.08$, $p\leq 0.05$). Event-triggered
365 averages of pupil diameter measurements were compared for the two conditions, real face-
366 to-face (Fig 4C) and video face/eye gaze (Fig 4D). While both groups initially showed pupil
367 dilation for gaze at real eyes, overall dilation in the ASD group was greater than in the TD
368 group ($p<0.05$). No evidence for differences was observed between groups during gaze at
369 the eyes in a video face suggesting increased autonomic responses to real faces, but not
370 video faces, in ASD (88).

371

Figure 4. A, B. Marginal means plots based on linear mixed effects models for each measure by participant group (Blue: Autism Spectrum Disorder (ASD) participants; Red: Typically-developed (TD) participants). **A.** Dwell time duration of eye contact on either the eyes in the video (Video Eye condition) or eyes of the lab partner (Real Eye condition). **B.** Standard deviation of horizontal gaze trajectory normalized by duration of contact. Error bars show SEM. *** $p \leq 0.001$, * $p \leq 0.05$. **C, D. Pupil diameter variations** observed in ASD and TD participants during Real Eye (**C**) and Video Eye (**D**) gaze conditions (Blue: Autism Spectrum Disorder (ASD) participants; Red: Typically-developed (TD) participants). Black lines indicate points at which pupil diameter differences between groups were significant at $p \leq 0.05$.

372 ***Neural Findings***

373 **Direct comparison of TD and ASD findings for real eye-to-eye contact.** A test of the
374 alternative neural pathways hypothesis for live and interactive face processing in ASD is
375 shown in Fig 5 with a direct comparison of the TD and ASD neural responses during live
376 eye-to-eye contact. Red clusters indicate increased neural activity for the TD group and blue
377 clusters indicate increased neural activity for the ASD ($p \leq 0.05$ FDR-corrected). Neural
378 activity in the Real Eye condition is increased in the dorsal parietal regions for TD > ASD and
379 in the temporal and ventral frontal regions for ASD > TD. See caption and tables for specific
380 anatomical details.

381

382

Figure 5. Contrast comparison [Real Eye > Rest], Typically-Developed (TD) participants relative to Autism Spectrum Disorder (ASD) participants. TD participants (red clusters) show comparatively greater activation in dorsal somatosensory cortex (SSC); supramarginal gyrus (SMG); angular gyrus (AG); pre- and supplementary motor cortex (MC); and extrastriate visual cortex (V3), while heightened activity was observed for ASD participants (blue clusters) in relatively ventral MC; SSC; pars opercularis (Pars O) and pars triangularis (Pars T); posterior middle temporal gyrus (pMTG); superior temporal gyrus (STG); and auditory cortex (AC). See Table 1. Yellow and light blue indicate responses corrected for multiple comparisons using FDR at $p \leq 0.05$. GLM analyses are based on the combined OxyHb and deOxyHb signals.

383

Table 1. GLM Contrast comparison: [Real Eye] > [Rest] (deOxyHb + OxyHb signals), TD group - ASD group

| Contrast | Contrast Threshold | Peak Voxels | | | | | df ² | Anatomical Regions in Cluster | Prob. ⁴ | | |
|----------------------------|--------------------|------------------------------|-------|-------|---------|-------------------------|-----------------|---|--------------------|--------------------------|-----|
| | | MNI Coordinates ¹ | | | t value | p | | | BA ³ | n of Voxels ⁵ | |
| [Real Eye> Rest] | p = 0.05 | 58 | -60 | 40 | 2.28 | 0.015 | 33 | Supramarginal Gyrus | 40 | 0.65 | 306 |
| | | | | | | | | Angular Gyrus | 39 | 0.35 | |
| | | 50 | -20 | 60 | 2.26 | 0.015 | 33 | Primary Somatosensory Cortex | 3 | 0.32 | 128 |
| | | | | | | | | Pre- and Supplementary Motor Cortex | 6 | 0.21 | |
| | | | | | | | | Primary Somatosensory Cortex | 1 | 0.17 | |
| | | | | | | | | Primary Somatosensory Cortex | 2 | 0.14 | |
| | | | | | | | | Primary Motor Cortex | 4 | 0.12 | |
| | | | | | | | | Extrastriate Visual Cortex (V3) | 19 | 1.00 | |
| | | 28 | -82 | 30 | 2.34 | 0.013 | 33 | Pars Triangularis | 45 | 0.30 | 495 |
| | | | | | | | | Pars Opercularis | 44 | 0.27 | |
| | | | | | | | | Pre- and Supplementary Motor Cortex | 6 | 0.21 | |
| | | | | | | | | Superior Temporal Gyrus | 22 | 0.13 | |
| | | | | | | | | Superior Temporal Gyrus | 22 | 0.32 | |
| | | 70 | -22 | 4 | -2.46 | 0.010 | 33 | Middle Temporal Gyrus | 21 | 0.31 | |
| | | | | | | | | Auditory Primary and Association Cortex | 42 | 0.31 | |
| Middle Temporal Gyrus | 21 | | | | | | | 0.57 | 92 | | |
| Superior Temporal Gyrus | 22 | | | | | | | 0.32 | | | |
| 68 | -42 | -2 | -2.25 | 0.015 | 33 | Middle Temporal Gyrus | 21 | 0.57 | 92 | | |
| | | | | | | Superior Temporal Gyrus | 22 | 0.32 | | | |
| | | | | | | Occipitotemporal Cortex | 37 | 0.12 | | | |

¹Coordinates are based on the MNI system and (-) indicates left hemisphere. ²df = degrees of freedom. ³BA = Brodmann Area. ⁴Probability of inclusion in cluster. ⁵"n of Voxels" refers to a relative index of cluster size on the rendered brain

384

385 **Modulation of neural circuitry by frequency of eye contact events.** A further test of the
386 ventral vs dorsal alternative pathways hypothesis is shown in Fig 6. Neural responses during
387 each 3 s eye viewing period were modulated by the number of eye contact events within
388 that period for both TD and ASD groups. The covariance variable of eye-contacts used in
389 the second level (group) analysis was constructed by assigning each subject with the
390 median eye contact time for the 3 s periods where the eye of the partner was viewed. For
391 TD participants (Fig 6A) clusters were observed in right dorsal supramarginal gyrus (SMG),
392 somatosensory association cortex (SSAC), and dorsolateral prefrontal cortex (DLPFC);
393 frontal eye fields (FEF); and pre- and supplementary motor cortex (MC) (see Table 2A). In
394 sharp contrast to these TD observations, ASD participants' (Fig 6B) neural responses to eye-
395 to-eye signals modulated by the same measures of eye contact events were observed in

396 the ventral right supramarginal gyrus (SMG); angular gyrus (AG); extrastriate visual (V3)
397 and visual association cortices (V2); as well as the dorsolateral prefrontal cortex (DLPFC).
398 Neural patterns in TD and ASD participants both demonstrated activity in the DLPFC
399 whereas group response patterns were clearly differentiated in the posterior regions of the
400 brain. In the case of TD participants, dorsal parietal regions were responsive to eye-to-eye
401 contact, while in the ASD participants, ventral occipital and temporal regions were
402 responsive to eye-to-eye contact. In summary, the findings are consistent with the
403 hypothesis of alternative neural pathways for live eye contacts between TD and ASD groups.
404 In particular, in TD the right dorsal parietal stream is activated, whereas in ASD, the right
405 ventral occipital-temporal stream is activated.

406

Figure 6. Contrast comparison [Real Eye] > [Rest] modulated by the number of frames within each 3-second eye viewing period where the gaze of both partners was simultaneously within the eye box of the other. A. Typically-developed (TD) participants. Activity observed in the right hemisphere: supramarginal gyrus (SMG); somatosensory association cortex (SSAC); dorsolateral prefrontal cortex (DLPFC); frontal eye fields (FEF); and pre- and supplementary motor cortex (MC). See Table 2A. Note: n = 15 rather than 19 (see Table S2) because eye tracking data could not be acquired on four participants. **B.** Autism Spectrum Disorder (ASD) participants. Activity observed in the right hemisphere include SMG; angular gyrus (AG); extrastriate visual cortex (V3); visual association cortex (V2); and DLPFC. See Table 2B. Note: n = 12 rather than 17 (see Table S1) because eye tracking data could not be acquired on five participants. Yellow indicates signals corrected for multiple comparisons at $p \leq 0.05$ using FDR. GLM analyses are based on the combined OxyHb and deOxyHb signals.

407

408

409

410

411

412

413

**Table 2A. GLM Contrast comparison: [Real Eye] > [Rest] with eye contact regressor
(deOxyHb + OxyHb signals), TD group**

| Contrast | | Peak Voxels | | | | | | | | | |
|----------------------------|-----------|------------------------------|-----|----|---------|--------|-----------------|-------------------------------------|-----------------------|-------------|-----|
| Contrast | Threshold | MNI Coordinates ¹ | | | t value | p | df ² | Anatomical Regions in Cluster | Prob. BA ³ | n of Voxels | |
| [Real Eye >Rest] | p = 0.05 | 58 | -54 | 48 | 3.78 | 0.0012 | 13 | Supramarginal Gyrus | 40 | 0.93 | 344 |
| | | 58 | 12 | 38 | 4.76 | 0.0002 | 13 | Dorsolateral Prefrontal Cortex | 9 | 0.52 | 342 |
| | | | | | | | | Pre- and Supplementary Motor Cortex | 6 | 0.30 | |
| | | | | | | | | Frontal Eye Fields | 8 | 0.16 | |
| | | 26 | -62 | 54 | 2.37 | 0.0170 | 13 | Somatosensory Association Cortex | 7 | 1.00 | 18 |
| | | 62 | -2 | 42 | 3.06 | 0.0045 | 13 | Pre- and Supplementary Motor Cortex | 6 | 0.82 | 10 |

¹Coordinates are based on the MNI system and (-) indicates left hemisphere. ²df = degrees of freedom. ³BA = Brodmann Area.

414

415

416

417

418

419

420

421

422

423

424

425

**Table 2B. GLM Contrast comparison: [Real Eye] > [Rest] with eye contact regressor
(deOxyHb + OxyHb signals), ASD group**

| Contrast | Contrast Threshold | Peak Voxels | | | | df ² | Anatomical Regions in Cluster | BA ³ | Prob. | n of Voxels | |
|------------------|--------------------|------------------------------|---------|----|------|-----------------|-------------------------------|---|-------|-------------|-----|
| | | MNI Coordinates ¹ | t value | p | | | | | | | |
| [Real Eye >Rest] | p = 0.05 | 54 | -72 | 22 | 5.73 | 0.0001 | 10 | Angular Gyrus | 39 | 0.69 | 544 |
| | | | | | | | | Extrastriate Visual Cortex (V3) | 19 | 0.29 | |
| | | 50 | -82 | 0 | 4.24 | 0.0008 | 10 | Extrastriate Visual Cortex (V3) | 19 | 0.67 | 536 |
| | | | | | | | | Visual Association Cortex (V2) | 18 | 0.23 | |
| | | 56 | 18 | 32 | 3.59 | 0.0025 | 10 | Dorsolateral Prefrontal Cortex | 9 | 0.58 | 195 |
| | | | | | | | | Pars Triangularis | 45 | 0.15 | |
| | | | | | | | | Dorsolateral Prefrontal Cortex | 46 | 0.13 | |
| | | 70 | -30 | 26 | 2.75 | 0.0102 | 10 | Supramarginal Gyrus | 40 | 0.53 | 191 |
| | | | | | | | | Auditory Primary and Association Cortex | 42 | 0.13 | |
| | | | | | | | | Superior Temporal Gyrus | 22 | 0.12 | |

¹Coordinates are based on the MNI system and (-) indicates left hemisphere. ²df = degrees of freedom. ³BA = Brodmann Area.

426

427 **Neural responses during real eye gaze modulated by symptom severity as measured**

428 **by ADOS-2: Group effects.** Neural responses (beta values) acquired during eye-gaze were

429 regressed by the individual ADOS-2 scores using the general linear model, GLM. The whole-

430 brain main effect of the eye contact activity modulated by ADOS-2 scores is shown in Fig 7.

431 Blue clusters indicate regions of the brain where neural activity as represented by the

432 individual average was negatively related to the individual ADOS-2 scores. That is,

433 participants with higher ADOS-2 scores and greater symptomatology showed consistently

434 lower live eye contact related neural activity located in the right dorsal parietal areas

435 including angular gyrus (AG), supramarginal gyrus (SMG), somatosensory association

436 cortex (SSAC), and somatosensory cortex (SSC). Similar findings were also observed the
 437 right dorsolateral prefrontal cortex (DLPFC) ($p \leq 0.01$). See Table 3.

Figure 7. Main effect neural results for Autism Spectrum Disorder (ASD) participants during real eye contact with ADOS-2 (Autism Diagnostic Observation Schedule, 2nd Edition) scores as a linear regressor. OxyHb and deOxyHb signals are combined. See Table 3. Blue colors indicate a negative relationship between neural responses and ADOS scores indicating that as symptom severity increases, neural responsiveness in these regions decreases. Light blue indicates responses corrected for multiple comparisons using FDR at $p \leq 0.01$. SSC: somatosensory cortex; SSAC: somatosensory association cortex; SMG: supramarginal gyrus; and AG: angular gyrus.

438

Table 3. GLM Contrast comparison: [Real Eye > Rest] with ADOS-2 regressor (deOxyHb + OxyHb signals)

| Contrast | Contrast Threshold | Peak Voxels | | | | | p | df ^b | Anatomical Regions in Cluster | Probability | n of Voxels |
|-------------------|--------------------|------------------------------|-----|----|---------|-----------------|---|----------------------------------|-------------------------------|-------------|-------------|
| | | MNI Coordinates ^a | | | t value | BA ^c | | | | | |
| [Real Eye > Rest] | p = 0.01 | 40 | -76 | 32 | -11.1 | 0.001 | 9 | Extrastriate Visual Cortex (V3) | 19 | 0.69 | 1016 |
| | | | | | | | | Angular Gyrus | 39 | 0.31 | |
| | | 52 | 28 | 36 | -5.28 | 0.001 | 9 | Dorsolateral Prefrontal Cortex | 9 | 0.51 | 442 |
| | | | | | | | | Dorsolateral Prefrontal Cortex | 46 | 0.30 | |
| | | | | | | | | Frontal Eye Fields | 8 | 0.16 | |
| | | 42 | -30 | 58 | -3.01 | 0.007 | 9 | Primary Somatosensory Cortex | 3 | 0.25 | 10 |
| | | | | | | | | Primary Somatosensory Cortex | 2 | 0.22 | |
| | | | | | | | | Primary Somatosensory Cortex | 1 | 0.19 | |
| | | | | | | | | Supramarginal Gyrus | 40 | 0.18 | |
| | | | | | | | | Primary Motor Cortex | 4 | 0.13 | |
| | | 36 | -34 | 60 | -3.08 | 0.007 | 9 | Primary Somatosensory Cortex | 2 | 0.27 | 10 |
| | | | | | | | | Primary Somatosensory Cortex | 3 | 0.20 | |
| | | | | | | | | Primary Somatosensory Cortex | 1 | 0.18 | |
| | | | | | | | | Primary Motor Cortex | 4 | 0.15 | |
| | | | | | | | | Somatosensory Association Cortex | 5 | 0.11 | |

^aCoordinates are based on the MNI system and (-) indicates left hemisphere. ^bdf = degrees of freedom. ^cBA = Brodmann Area.

439

440 **Neural responses during real eye gaze correlated with symptom severity as measured**
 441 **by ADOS-2: Individual ASD effects.** The individual ADOS-2 scores for each participant
 442 (identified by participant number in Table S1) (x-axis) are plotted against the median beta-
 443 values, parameter estimations, of the fNIRS signal (y-axis) for the two regions of interest
 444 identified by the group effects above: A posterior dorsal stream cluster consisting of the
 445 somatosensory association cortex, supramarginal gyrus, angular gyrus, and somatosensory

446 cortex, and an anterior cluster in the dorsolateral prefrontal cortex. The best fit lines illustrate
447 the negative relationships for the posterior regions ($r = -0.69$, Fig 8A) and anterior frontal
448 area ($r = -0.77$, Fig 8B).

Figure 8. Autism Spectrum Disorder (ASD) participants (numbers correspond to Table S1) during eye contact beta values vs. ADOS-2 (Autism Diagnostic Observation Schedule, 2nd Edition) scores. The median hemodynamic signals (Beta values, y-axis) within the responsive brain regions (Fig 7 and Table 3) and ADOS-2 scores (x-axis) are shown for each participant. The main effect of eye-to-eye contact is negatively correlated with fNIRS signals in **A.** right hemisphere somatosensory association cortex, supramarginal gyrus, angular gyrus, and somatosensory cortex ($r = -0.69$); and **B.** right dorsolateral prefrontal cortex ($r = -0.77$).

449

450 **Neural responses during real eye gaze correlated with symptom severity as measured**

451 **by SRS-2: Individual ASD and TD Effects.** To further evaluate the relationship between

452 social symptomatology and live-face eye-gaze for ASD and TD participants we combine the

453 SRS-2 scores for both groups based on the assumption that ASD traits are also present in

454 the general population. Consistent with the findings based on the ADOS-2 scores above, a

455 negative relationship (blue cluster in Fig 9) was observed in regions located in the right

456 dorsal stream including somatosensory cortex (SSC), somatosensory association cortex

457 (SSAC), and supramarginal gyrus (SMG). Participants with higher SRS-2 scores indicating

458 higher levels of symptomatology showed reduced neural activity during eye contact in the

459 right somatosensory cortex (SSC), somatosensory association cortex (SSAC), and

460 supramarginal gyrus (SMG) ($p \leq 0.01$). Table 4 provides the peak MNI coordinates, cluster t-

461 values, anatomical regions within the cluster, Brodmann's Area (BA), probability of inclusion

462 in the cluster, and relative size of the active area (n of voxels).

Figure 9. Main effect neural results for Autism Spectrum Disorder (ASD) and typically-developed (TD) participants during eye contact with SRS-2 (Social Responsiveness Scale, Second Edition) scores as a linear regressor. OxyHb and deOxyHb signals are combined. Blue colors indicate a negative relationship between neural responses and SRS-2 scores, which suggests that increased symptom severity is associated with reduced regional neural responsiveness (See Table 4). Light blue indicates responses corrected for multiple comparisons using FDR at $p \leq 0.01$. SSC: somatosensory cortex, SSAC: somatosensory association cortex, and SMG: supramarginal gyrus.

463

Table 4. GLM Contrast comparison: [Real Eye>Rest] with SRS-2 regressor (deOxyHb + OxyHb signals)

| Contrast | Contrast Threshold | Peak Voxels | | | | | | Anatomical Regions in Cluster | BA ^c | Probability | n of Voxels | |
|-------------------|--------------------|------------------------------|-----|----|---------|-------|---------------------|----------------------------------|-------------------------------------|-------------|-------------|--|
| | | MNI Coordinates ^a | | | t value | p | df ^b | | | | | |
| [Real Eye > Rest] | p = 0.01 | 10 | -64 | 60 | -3.45 | 0.001 | 25 | Somatosensory Association Cortex | 7 | 1.00 | 147 | |
| | | 28 | -44 | 64 | -2.98 | 0.003 | 25 | Somatosensory Association Cortex | 5 | 0.47 | 53 | |
| | | | | | | | | | Somatosensory Association Cortex | 7 | 0.23 | |
| | | | | | | | | | Primary Somatosensory Cortex | 2 | 0.20 | |
| | | 48 | -24 | 60 | -2.71 | 0.006 | 25 | Primary Somatosensory Cortex | 3 | 0.30 | 47 | |
| | | | | | | | | | Primary Somatosensory Cortex | 1 | 0.17 | |
| | | | | | | | | | Primary Somatosensory Cortex | 2 | 0.16 | |
| | | | | | | | | | Primary Motor Cortex | 4 | 0.13 | |
| | | | | | | | | | Pre- and Supplementary Motor Cortex | 6 | 0.13 | |
| | | | | | | | Supramarginal Gyrus | 40 | 0.12 | | | |

^aCoordinates are based on the MNI system and (-) indicates left hemisphere. ^bdf = degrees of freedom. ^cBA = Brodmann Area.

464

465

466 **SRS-2 scores and neural responses: Individual Differences.** The individual SRS-2
 467 scores for each participant (identified by a number that corresponds to the participant
 468 number in Tables S1 and S2) are plotted against the individual median beta values of the
 469 fNIRS signal (Fig 10). Red numbers represent TD participants and blue numbers represent
 470 ASD participants. The interspersal of the individual scores between ASD and TD participants
 471 is consistent with the assumption that social responsiveness traits vary within the general

472 population as well as within ASD. The best fit line illustrates the negative relationship ($r = -$
473 0.58).

Figure 10. Autism Spectrum Disorder (ASD) participants (blue numbers) and typically-developed (TD) participants (red numbers) during eye contact vs. Social Responsiveness Scale (Second Edition, SRS-2) scores. The median hemodynamic signals (Beta values, y-axis) within the responsive brain region (Fig 9 and Table 4) and SRS-2 scores (x-axis) are shown for each participant. The main effect of eye-to-eye contact is negatively correlated with fNIRS signals in right hemisphere somatosensory cortex, somatosensory association cortex, and dorsal supramarginal gyrus ($r = -0.58$). Numbers indicate individual participants shown in Table S1 (ASD participants) and Table S2 (TD participants).

474

475 **Discussion**

476 **Summary of findings.** Overall, there were three main findings of this investigation: 1) the
477 alternative neural processes hypothesis was supported for live and interactive faces in ASD.
478 Specifically, neural systems within ventral occipital-temporal regions were engaged
479 d in ASD whereas in TD these functions were associated with dorsal parietal and lateral
480 prefrontal regions; 2) Variations in oculomotor and visual sensing were observed in ASD
481 including increased positional variation in eye fixations and increased pupillary reactions to
482 live faces, suggesting that visual acquisition factors may also contribute to live face
483 processing mechanisms; and 3) A biological basis for social performance associated with
484 ASD is suggested by the association between ADOS-2 and SRS-2 scores and the counter-
485 correlation of neural responses in the right dorsal parietal regions during real eye-to-eye
486 contact.

487 Differences in social performance, including reduced eye contact, are common
488 characteristics of ASD. Although disparities in face processing and oculomotor variations in
489 ASD are well documented, it is not known how these behaviors are linked to the underlying
490 neurophysiology associated with live and natural interactions. In this investigation, we
491 employed a two-person paradigm using functional near-infrared spectroscopy (fNIRS) to
492 acquire neuroimaging responses during live dynamic eye-to-eye contacts with a lab partner

493 that are a close proxy to the behaviors under investigation. Simultaneous eye-tracking and
494 oculomotor responses were also acquired in 17 adult ASD dyads and 19 closely matched
495 TD adult dyads. Social performance was quantified by clinical interview (ADOS-2: Autism
496 Diagnostic Observation Schedule, 2nd Edition) in ASD and self-report (SRS-2: Social
497 Responsiveness Scale, Second Edition) in both ASD and TD to test the hypothesis that
498 individual differences in social function are predicted by neural responses associated with
499 live eye-to-eye contact.

500 Direct comparisons of neural findings between TD and ASD for the Real Eye
501 condition are consistent with right dorsal parietal activity in the case of TD (TD > ASD) and
502 right ventral occipital-temporal activity in the case of ASD (ASD > TD). Neural findings
503 modulated by real eye-to-eye contact behavior revealed similar findings of increased right
504 dorsal parietal activity for TD and alternatively increased right ventral parietal activity for ASD
505 consistent with the hypothesis of dorsal eye processing systems for TD and ventral eye
506 processing streams for ASD groups. Individual ADOS-2 scores were negatively correlated
507 ($r = -0.69$) with individual fNIRS beta values (representing the strength of hemodynamic
508 signals) within clusters in the right dorsal parietal stream including somatosensory cortices,
509 angular gyrus, and supramarginal gyrus. Similarly, SRS-2 scores for the combined ASD and
510 TD groups were negatively correlated ($r = -0.58$) with somatosensory cortices and the
511 supramarginal gyrus also located in the right dorsal parietal stream. Since these two clinical
512 measures provide similar information, it is expected that their relationship to underlying
513 neural correlates would be similar. Neural responses in the right dorsolateral prefrontal
514 cortex (DLPFC) during live eye-to-eye contact were also negatively correlated ($r = -0.77$)
515 with ADOS-2 scores. These correlations between social function and the neural responses
516 during live eye-to-eye contact are consistent with a model of dorsal parietal and dorsal lateral
517 prefrontal cortex contributing to behavioral differences in ASD.

518 ***Two-person Visual Sensing in ASD***

519 Pupilometry, a presumed measure of activity associated with the locus coeruleus-
520 norepinephrine system (88) revealed increased pupil diameters for ASD during real eye
521 conditions but not the video eye conditions relative to TD ($p < 0.05$), consistent with the
522 interpretation of increased arousal associated with the real face and eyes. Further, variance
523 of gaze positions was greater for ASD than TD for both real and video faces suggesting
524 oculomotor differences in visual sensing (89).

525 A natural in-person encounter typically involves active visual sensing of dynamic face
526 landmarks (90). Guidance systems for visual saccades and fixations are thought to actively
527 “seek” relevant visual information such as social cues that are conveyed hierarchically to
528 higher levels of neural processing (89). The cascade of synchronized oculomotor behaviors,
529 for example, associated with mutual live eye-to-eye contacts does not occur during passive
530 gaze at an inanimate representation of a real person because dynamic behaviors from both
531 partners are required for a mutual eye contact event or a dynamic face-to-face interaction.
532 In this investigation, we include measures of visual sensing, dwell time, and positional
533 variance as well as pupil size to test the hypothesis that in ASD the live two-person condition
534 may be distinguished by oculomotor behaviors in addition to neural processing. Differences
535 in oculomotor functions have been previously reported in ASD, for example, for static and
536 simulated stimuli (91, 92). Here we test the hypothesis that oculomotor systems are also
537 affected during two-person face-to-face interactions.

538 The observed increased positional variation in ASD eye movements leads to the
539 speculation that information characterizing an interactive face may not have been sufficiently
540 acquired for ASD participants. The finding that live face processing in the ASD group
541 increased activity in ventral and lateral occipital and temporal regions, rather than dorsal
542 parietal regions, could be due, in part, to differences in visual sensing. The observed ventral

543 processes are more consistent with non-interactive face functions than with interactive
544 functions. For example, topographical maps associated with regional specializations for
545 coding simulated faces are well-established. The ventral-occipital cortex is highly selective
546 for and sensitive to pictures of faces (93, 94). Regions within the superior temporal sulcus
547 are involved in detecting dynamic facial movements presented in two-dimensional stimuli
548 (27, 29), and parameterized face processing codes for static faces have been identified by
549 electrophysiology in middle and superior temporal gyri of non-human primates (95).

550 ***Live Two-Person Interactions in ASD***

551 Neuroimaging based on functional near-infrared spectroscopy (fNIRS) enables
552 simultaneous acquisition of hemodynamic brain signals from two individuals (hyperscanning)
553 dynamically engaged in natural interactions. Eye tracking acquired simultaneously on both
554 participants during face-to-face engagement enables identification of eye contact events that
555 occur between the partners. The aim to understand the neural mechanisms that underlie
556 social function in ASD has motivated this multi-modal application of fNIRS and eye tracking.
557 In spite of the biological significance of live interpersonal interactions for survival and social
558 well-being, the underlying neural processes of interactive behaviors are relatively novel
559 targets of investigation for natural settings as well as clinical, developmental, and psychiatric
560 applications (37-39, 96). Fundamental models of dynamic and reciprocal behaviors are
561 under development for multiple sensory and communication systems, clinical applications,
562 and social behaviors (37-39, 97-102).

563 Current models of face and eye processing in TD and ASD are based primarily on
564 non-interactive paradigms where data are acquired in single-subject situations using
565 conventional stimulus and response models rather than dyadic paradigms that include live
566 social interactions. The importance of investigations that include natural and dynamic two-
567 person interactions between individuals is highlighted by a general theoretical framework

568 proposed by the Interactive Brain Hypothesis (103, 104), which suggests that live
569 interactions between individuals engage neural functions not activated during similar tasks
570 performed alone, i.e., without interaction. A rapidly emerging neuroimaging literature and
571 theoretical framework of live and natural interactions compared to single-subject interactions
572 contributes an accumulating body of evidence in support of this hypothesis (31, 37, 39, 40,
573 67, 102, 105). Understanding neural activity during natural interactions is especially critical
574 in ASD, as the defining social and communicative characteristics of the condition are often
575 attenuated or absent during explicit laboratory tasks (41).

576 This long-standing experimental paucity of two-person interactive experimental
577 paradigms in ASD, in part, reflects the historical limitations of conventional neuroimaging
578 methods. For example, in functional magnetic resonance imaging (fMRI) solitary
579 confinement in the bore of a scanner with minimal tolerance of head movements
580 constrains/contra-indicates investigations of natural, two-person interactions. Fortunately,
581 however, these particular limitations are substantially resolved by recent developments of
582 optical neuroimaging, functional near-infrared spectroscopy (fNIRS), a non-invasive spectral
583 absorbance technique that detects changes in blood oxygen levels in both oxyhemoglobin
584 and deoxyhemoglobin using surface-mounted optical sensors (106-109). Functional NIRS
585 enables simultaneous acquisitions of hemodynamic signals (assumed to be a proxy for
586 neural activity as in fMRI) from naturally interacting dyads and provides simultaneous dyadic
587 measures that contribute to understanding interactive behaviors as opposed to single-
588 subject responses that focus primarily on perceptual and cognitive systems.

589 ***Social performance and face processing***

590 This application of two-person neuroimaging technology to investigate the
591 relationship between the neural underpinnings of interactive face and eye contact and social
592 performance in ASD addresses a prominent and understudied question. Individual clinical
593 evaluations of social performance applied as a second level regressor on whole-brain
594 neuroimaging findings acquired during live real person eye-to-eye contacts confirm a
595 negative relationship between test scores and neural signals in brain regions responsive to
596 real eye-to-eye contacts. Participants with higher ADOS-2 scores, reflecting reduced social
597 performance, showed lower neural signals (beta values, an indicator of signal strength and
598 fit to the general linear model) in brain regions previously associated with social activity,
599 interactive face processing, and motion sensitivity. Findings also included the right
600 dorsolateral prefrontal cortex, a region implicated in both ASD and commonly co-occurring
601 conditions, such as major depressive disorder. Further, a similar finding was observed for
602 the SRS-2 when the scores of both TD and ASD participants were combined for regions
603 within the dorsal stream but not the DLPFC. That is, as individual social ability decreased
604 as indicated by the elevated SRS-2, the neural signal decreased in the right dorsal-stream
605 regions. A similar finding was observed for SRS-2 scores and the relationship to neural
606 signals acquired by fMRI in the fusiform gyrus and the amygdala during static face
607 processing (110). Interestingly, in this study, the SRS-2 finding included TD as well as ASD
608 participants suggesting that variations in social responsiveness and the associated
609 reduction in dorsal stream activity are similarly represented in the general population.

610 Unique features of this study include the live interactive eye-to-eye task as well as
611 the eye-tracking documentation of compliance combined with the individual difference
612 approach to characterize single participants by both measures. All data were acquired during
613 the epochs when participants directed their eye gaze to within the eye-box of the lab partner.

614 Continuous monitoring confirmed high levels of compliance in all cases. That is, when asked
615 to perform the task, participants were able to do it although eye-to-eye contact was not
616 necessarily a comfortable task for them.

617 These findings of a negative association between right dorsal regions and social
618 performance do not imply a causal role between neural substrates and reduced social
619 function. However, it can be concluded that the dorsal regions found to be related to
620 symptomatology (right hemisphere angular gyrus, supramarginal gyrus, somatosensory
621 association cortex, somatosensory cortex, and dorsolateral prefrontal cortex), are involved
622 in the underlying neural conditions relevant to ASD. Given a well-recognized need for
623 biomarkers for ASD that associate with the clinical phenotype at the individual level, the
624 strong relationships observed between neural activity and both clinician and self-reported
625 social function suggest potential utility in key contexts of use, such as stratification for
626 enrichment of clinical trials (111).

627 In conclusion, these findings highlight the right dorsal stream system and interactive
628 face processing as regions and tasks of interest for understanding the underlying neural
629 mechanisms that distinguish ASD and TD participants. The specificity of these findings
630 opens new directions for investigating these brain-to-behavior linkages. For example, these
631 regions have previously been implicated in motion sensitivity (48) and raise the interesting
632 hypothesis that reduced face processing in social interactions in ASD is related to reduced
633 sensitivity to the subtle expressive movements of a real face. However, the strong ($r = -0.77$)
634 negative correlation between social performance (ADOS-2) and the dorsolateral prefrontal
635 cortex in ASD does not fall under that hypothesis and was not predicted. These findings,
636 however, are consistent with face processing activity observed in right lateral prefrontal
637 cortex using fMRI and TD participants (112). Interestingly, in that study it was found that
638 face processing activity observed in the right inferior frontal junction (including regions

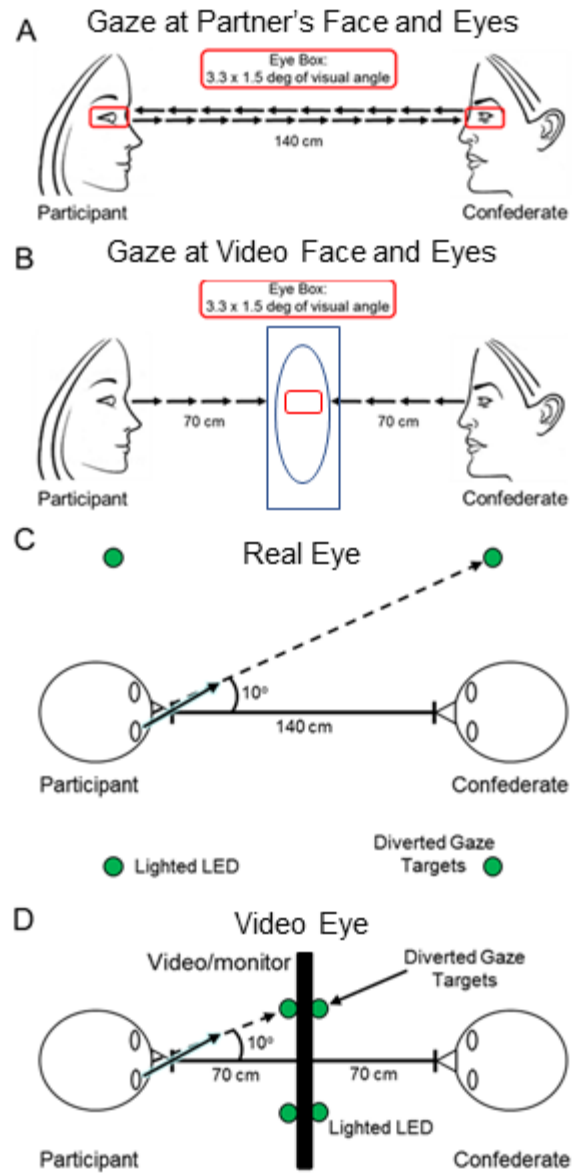
639 labeled as DLPFC and frontal eye fields, see Table 3) was primarily responsive to the eyes
640 and not the whole face. Consistent with these prior findings, in the study reported here the
641 strongest negative correlation between ADOS-2 scores and neural activity (-0.77) was in
642 this area and observed during eye contact (Figs 7 and 8). These findings suggest another
643 target of further investigation in this dorsal neural pathway and its role in social performance.

644 Within this framework, our findings are consistent with the hypothesis that eye
645 movements (increased positional variation) during live eye contact and social processing
646 are altered in ASD and suggest that “bottom-up” factors may also impact live eye-to-eye
647 interactions. Altered incoming information due to visual sensing factors such as increased
648 fixation variability could fail to capture higher-order motion cues associated with face and
649 social interactions. Individuals with ASD show raised thresholds for the perception of
650 coherent motion (10, 15, 113). These findings also add support for the “dorsal stream
651 vulnerability” hypothesis in ASD suggesting that mechanisms supporting motion sensitivity
652 such as live face interactions are compromised (48).

653 ***Limitations***

654 The advantages of fNIRS are balanced by technical limitations relative to fMRI. The
655 spatial resolution of fNIRS (approximately 3 cm) does not allow for discrimination of small
656 anatomical differences in functional activity between gyri, and the origin of acquired signals
657 does not extend below the superficial grey matter of the cortex of about 1.5-2.0 cm. Thus,
658 findings of this, and other investigations based on fNIRS technology, are restricted to
659 superficial cortical networks. Although the eye-to-eye contact occurs in a live context which
660 is a novel advance, the gaze situation in the study is relatively constrained which is
661 necessary for experimental control and thus also sets constraints on the investigation of
662 naturally occurring behaviors.

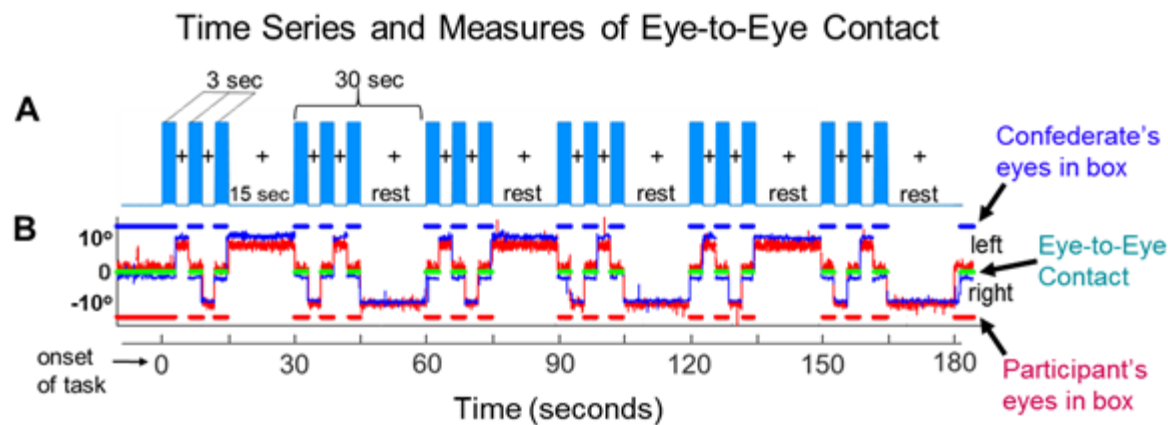
663



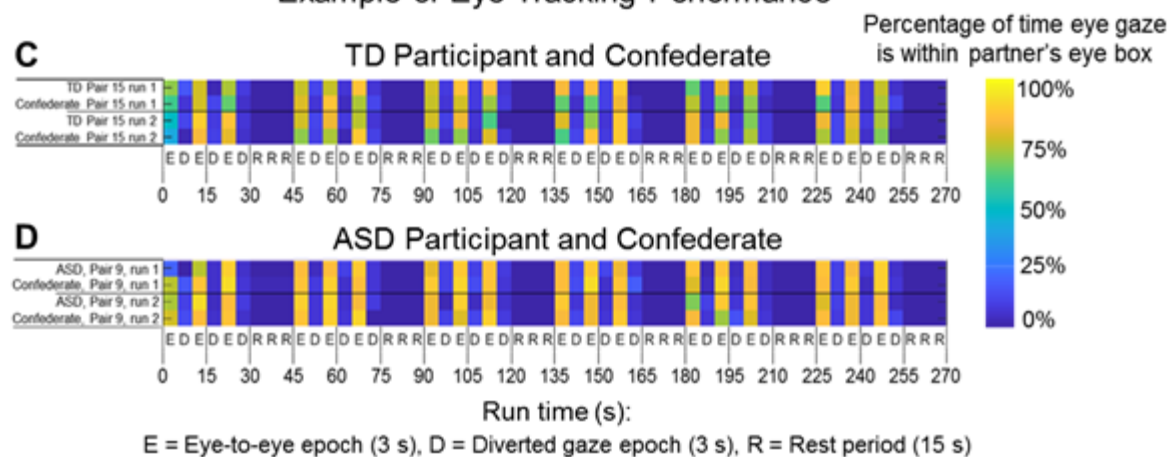
664

665 **Fig 1**

666



Example of Eye Tracking Performance

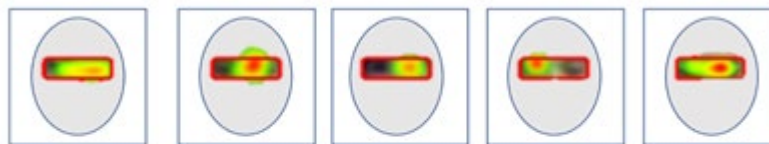


667

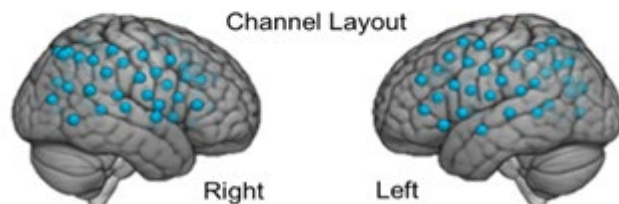
668 **Fig 2**

669

A. Illustration of Average Gaze position of participant on face of confederate

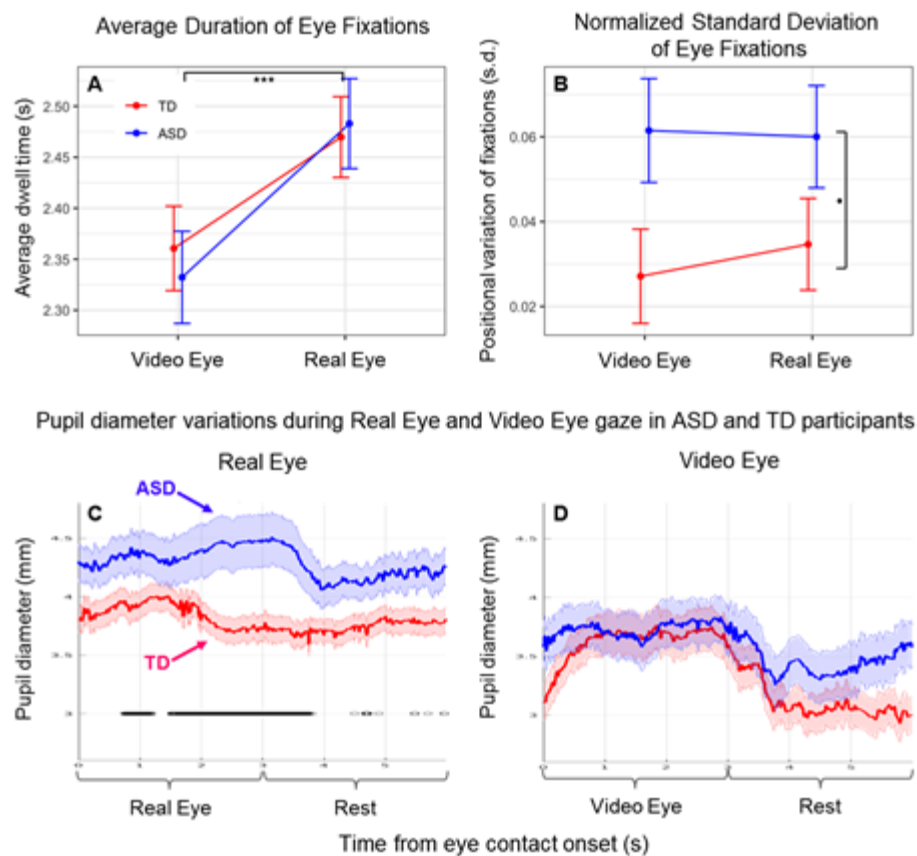


B.



670

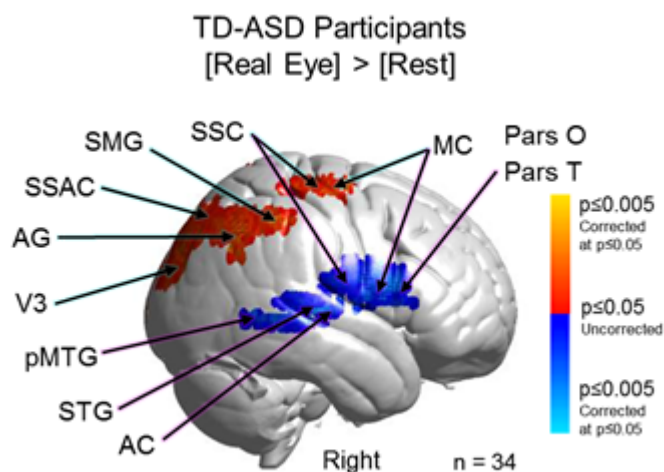
671 **Fig 3**



672

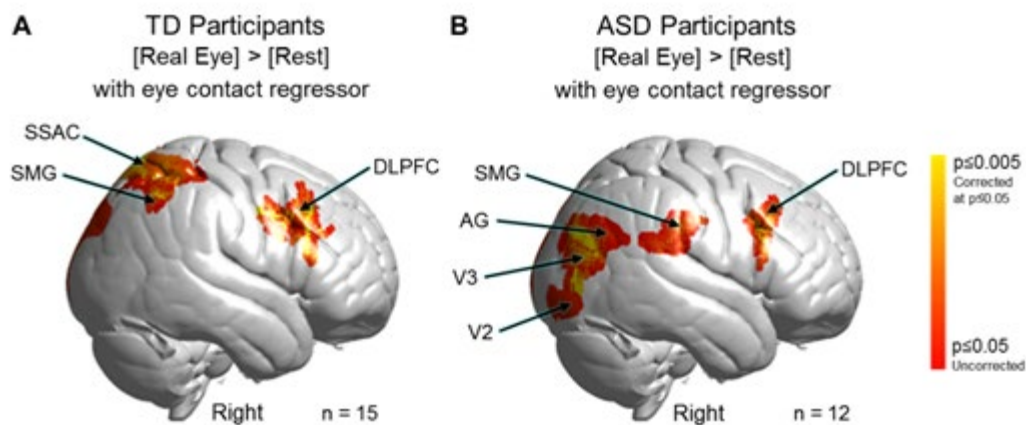
673 **Fig 4**

674



675

676 **Fig 5**



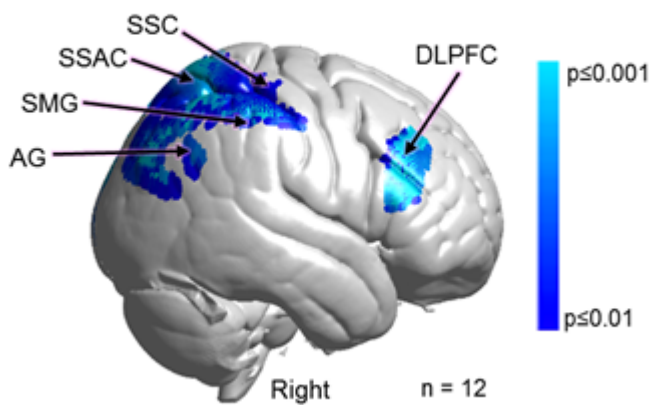
677

678 **Fig 6**

679

680

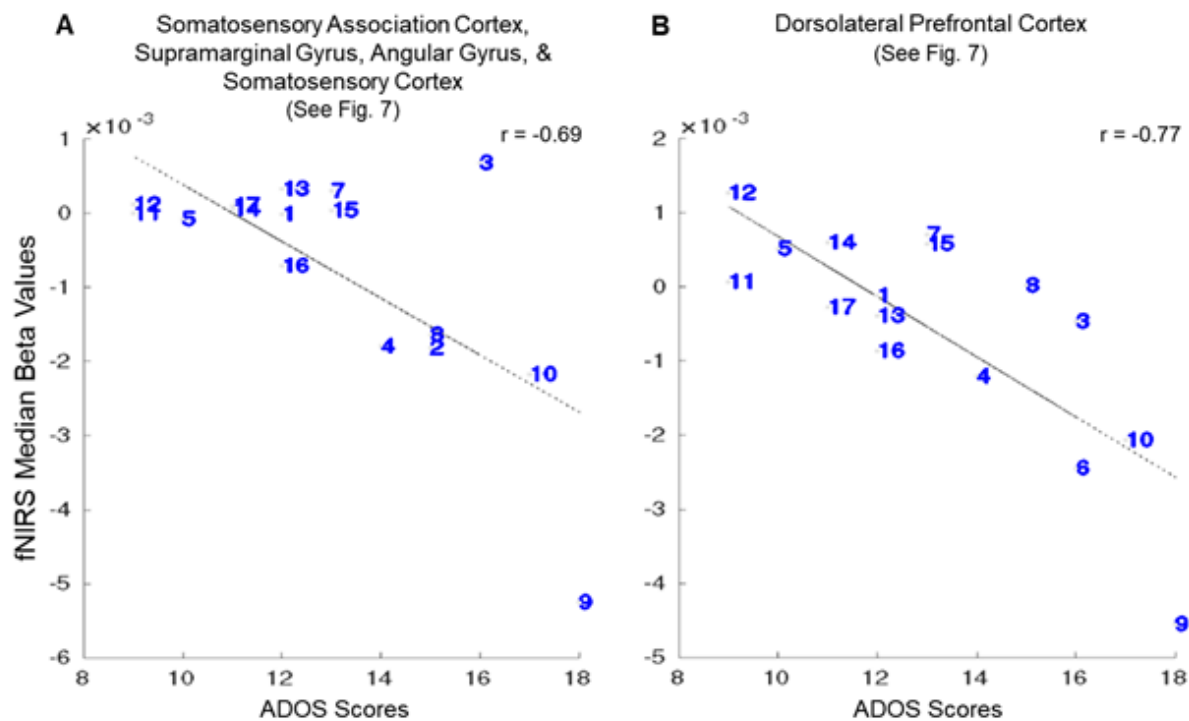
ASD Participants during eye contact with ADOS-2 regressor



681

682 **Fig 7**

ASD Participants during eye contact Median Beta Values vs. ADOS Scores by Region

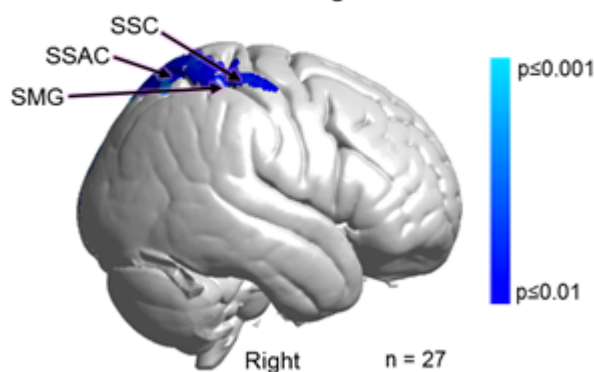


683

684 **Fig 8**

685

ASD and TD Participants during eye contact with SRS-2 regressor



686

687 **Fig 9**

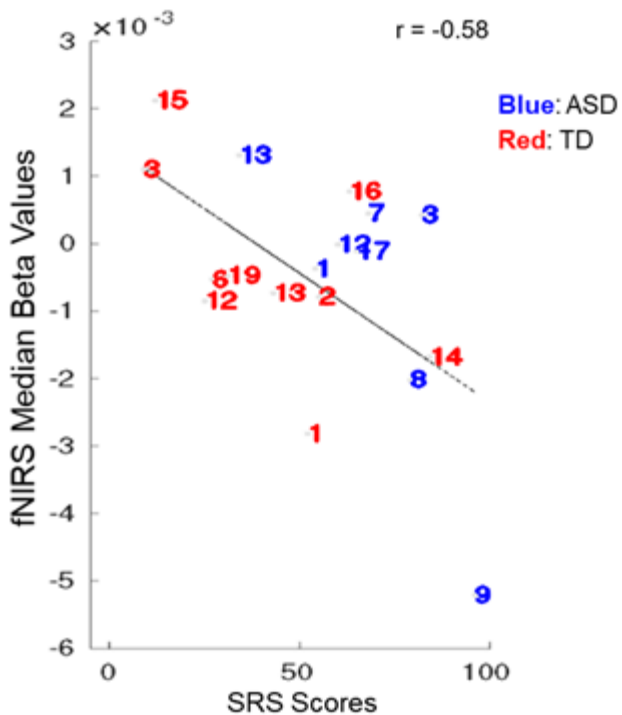
688

689

ASD and TD participants during eye contact

Median Beta Values vs. SRS Scores

Somatosensory Cortex,
Somatosensory Association Cortex,
and Supramarginal Gyrus
(See Figure 9)



690

691 **Fig 10**

692

693

694

695

696

697

698 **Author Information and Contributions**

699 Full Name: Joy Hirsch, PhD

700 Postal Address: Yale School of Medicine, Brain Function Laboratory, 300 George St,
701 Suite 902, New Haven, CT, 06511

702 Telephone Number: 917.494.7768

703 Email Address: joy.hirsch@yale.edu

704 Contribution(s): Research design and supervision; data analysis; wrote the paper

705 Full Name: James C. McPartland, PhD

706 Postal Address: Yale Child Study Center, Nieson Irving Harris Building, 230 South
707 Frontage Road, Floor G, Suite 100A, New Haven, CT, 06519

708 Telephone Number: 203.785.7179

709 Email Address: james.mcpartland@yale.edu

710 Contribution(s): Research design and clinical supervision; edited the paper

711 Full Name: Xian Zhang, PhD

712 Postal Address: Yale School of Medicine, Department of Psychiatry, Brain Function
713 Laboratory, 300 George St, Suite 902, New Haven, CT, 06511

714 Telephone Number: 917.494.7768

715 Email Address: xian.zhang@yale.edu

716 Contribution(s): Analysis of neuroimaging and eye tracking data; edited the paper

717 Full Name: J. Adam Noah, PhD

718 Postal Address: Yale School of Medicine, Department of Psychiatry, Brain Function
719 Laboratory, 300 George St, Suite 902, New Haven, CT, 06511

720 Telephone Number: 917.494.7768

721 Email Address: adam.noah@yale.edu

722 Contribution(s): Performed neuroimaging and eye tracking research; analyzed
723 neuroimaging data; maintenance of system calibrations and performance; edited the
724 paper

725

726 Full Name: Swethasri Dravida, MD-PhD

727 Postal Address: Yale School of Medicine, Brain Function Laboratory, 300 George St,
728 Suite 902, New Haven, CT, 06511

729 Telephone Number: 917.494.7768

730 Email Address: swethasri.dravida@yale.edu

731 Contribution(s): Data acquisition and analysis

732 Full Name: Adam Naples, PhD

733 Postal Address: Yale Child Study Center, Nieson Irving Harris Building, 230 South
734 Frontage Road, Floor G, Suite 100A, New Haven, CT, 06519

735 Telephone Number: 203.785.7179

736 Email Address: adam.naples@yale.edu

737 Contribution(s): Research design and clinical supervision

738 Full Name: Mark Tiede, PhD

739 Postal Address: Haskins Laboratories, 300 George St, 9th Floor, New Haven, CT, 06511

740 Telephone Number: 203.865.6163

741 Email Address: mark.tiede@yale.edu

742 Contribution(s): Analysis of eye tracking data and manuscript editing

743 Full Name: Julie M. Wolf, PhD

744 Postal Address: Yale Child Study Center, Nieson Irving Harris Building, 230 South
745 Frontage Road, New Haven, CT, 06519

746 Telephone Number: 203.785.5337

747 Email Address: julie.wolf@yale.edu

748 Contribution(s): Acquired and analyzed clinical data

749

750 **Acknowledgements**

751 The content is solely the responsibility of the authors and does not necessarily represent the
752 official views of the National Institutes of Health. All data reported in this paper are available
753 upon request from the corresponding and first author. The authors are grateful to the
754 participants for their essential efforts to advance understanding of ASD; to our two lab
755 partners, CD and IS, for consistent partnership with our participants and the investigators;
756 and to Jen Cuzzocreo for database management and graphical representations of the data.

757 **Disclosure of Biomedical Financial Interests and Potential Conflicts of Interest**

758 The authors declare that this research was conducted in the absence of any commercial or
759 financial relationships that could be construed as a potential conflict of interest.

760 **Data Availability Statement**

761 The datasets analyzed for this study will be made available upon request at fmri.org/
762 [ENDAR](#) and the NIH Data Archive.

763

References

- 764 1. Cicero MT. Orator (Chapter 18, Section 60). In: Wilkins AS, editor. Oxford Classical
765 Texts: M Tulli Ciceronis, Rhetorica. Oxford, England: Oxford University Press; 46 BC.
- 766 2. Ewbank MP, Jennings C, Calder AJ. Why are you angry with me? Facial
767 expressions of threat influence perception of gaze direction. *Journal of Vision*.
768 2009;9(12):16.
- 769 3. Matsumoto D, Consolacion T, Yamada H, Suzuki R, Franklin B, Paul S, et al.
770 American-Japanese cultural differences in judgements of emotional expressions of
771 different intensities. *Cognition & Emotion*. 2002;16(6):721-47.
- 772 4. Akechi H, Senju A, Uibo H, Kikuchi Y, Hasegawa T, Hietanen JK. Attention to eye
773 contact in the West and East: Autonomic responses and evaluative ratings. *PLoS ONE*.
774 2013;8(3):e59312.
- 775 5. Uono S, Hietanen JK. Eye contact perception in the west and east: A cross-cultural
776 study. *PLoS ONE*. 2015;10(2):e0118094.
- 777 6. American Psychiatric Association. Diagnostic and Statistical Manual of Mental
778 Disorders (DSM-5®). Washington, D.C.: American Psychiatric Association; 2013.
- 779 7. Nation K, Penny S. Sensitivity to eye gaze in autism: Is it normal? Is it automatic? Is
780 it social? *Development and Psychopathology*. 2008;20(1):79-97.
- 781 8. Bookheimer SY, Wang AT, Scott A, Sigman M, Dapretto M. Frontal contributions to
782 face processing differences in autism: Evidence from fMRI of inverted face processing.
783 *Journal of the International Neuropsychological Society*. 2008;14(6):922-32.
- 784 9. Constantino JN, Kennon-McGill S, Weichselbaum C, Marrus N, Haider A, Glowinski
785 AL, et al. Infant viewing of social scenes is under genetic control and is atypical in autism.
786 *Nature*. 2017;547(7663):340-4.
- 787 10. Pelphrey KA, Morris JP, McCarthy G. Neural basis of eye gaze processing deficits
788 in autism. *Brain*. 2005;128(5):1038-48.

- 789 11. Schneier FR, Kent JM, Star A, Hirsch J. Neural circuitry of submissive behavior in
790 social anxiety disorder: A preliminary study of response to direct eye gaze. *Psychiatry*
791 *Research: Neuroimaging*. 2009;173(3):248-50.
- 792 12. Senju A, Johnson MH. Atypical eye contact in autism: Models, mechanisms and
793 development. *Neuroscience & Biobehavioral Reviews*. 2009;33(8):1204-14.
- 794 13. McPartland JC, Webb SJ, Keehn B, Dawson G. Patterns of visual attention to faces
795 and objects in autism spectrum disorder. *Journal of Autism and Developmental Disorders*.
796 2011;41(2):148-57.
- 797 14. Jones W, Klin A. Attention to eyes is present but in decline in 2-6-month-old infants
798 later diagnosed with autism. *Nature*. 2013;504(7480):427.
- 799 15. Pelphrey KA, Sasson NJ, Reznick JS, Paul G, Goldman BD, Piven J. Visual
800 scanning of faces in autism. *Journal of Autism and Developmental Disorders*.
801 2002;32(4):249-61.
- 802 16. Rahko JS, Paakki J-J, Starck TH, Nikkinen J, Pauls DL, Kätsyri JV, et al. Valence
803 scaling of dynamic facial expressions is altered in high-functioning subjects with autism
804 spectrum disorders: an fMRI study. *Journal of autism and developmental disorders*.
805 2012;42(6):1011-24.
- 806 17. Chawarska K, Klin A, Volkmar F. Automatic attention cueing through eye movement
807 in 2-year-old children with autism. *Child Development*. 2003;74(4):1108-22.
- 808 18. Uljarevic M, Hamilton A. Recognition of emotions in autism: a formal meta-analysis.
809 *Journal of autism and developmental disorders*. 2013;43(7):1517-26.
- 810 19. Campbell R, Lawrence K, Mandy W, Mitra C, Jeyakuma L, Skuse D. Meanings in
811 motion and faces: Developmental associations between the processing of intention from
812 geometrical animations and gaze detection accuracy. *Developmental Psychopathology*.
813 2006;18(1):99-118.
- 814 20. Dawson G, Webb SJ, McPartland J. Understanding the nature of face processing
815 impairment in autism: Insights from behavioral and electrophysiological studies.
816 *Developmental Neuropsychology*. 2005;27(3):403-24.

- 817 21. Tanabe HC, Kosaka H, Saito DN, Koike T, Hayashi MJ, Izuma K, et al. Hard to
818 “tune in”: Neural mechanisms of live face-to-face interaction with high-functioning autistic
819 spectrum disorder. *Frontiers in Human Neuroscience*. 2012;6:268.
- 820 22. Tottenham N, Hertzog ME, Gillespie-Lynch K, Gilhooly T, Millner AJ, Casey B.
821 Elevated amygdala response to faces and gaze aversion in autism spectrum disorder.
822 *Social Cognitive and Affective Neuroscience*. 2014;9(1):106-17.
- 823 23. McPartland J, Cheung CH, Perszyk D, Mayes LC. Face-related ERPs are
824 modulated by point of gaze. *Neuropsychologia*. 2010;48(12):3657-60.
- 825 24. McPartland J, Dawson G, Webb SJ, Panagiotides H, Carver LJ. Event-related brain
826 potentials reveal anomalies in temporal processing of faces in autism spectrum disorder.
827 *Journal of Child Psychology and Psychiatry*. 2004;45(7):1235-45.
- 828 25. Jung CE, Strother L, Feil-Seifer DJ, Hutsler JJ. Atypical asymmetry for processing
829 human and robot faces in autism revealed by fNIRS. *PLoS One*. 2016;11(7):e0158804.
- 830 26. Parker TC, Crowley MJ, Naples AJ, Rolison MJ, Wu J, Trapani JA, et al. The N170
831 event-related potential reflects delayed neural response to faces when visual attention is
832 directed to the eyes in youths with ASD. *Autism Research*. 2021;14:1– 10.
- 833 27. Puce A, Allison T, Bentin S, Gore JC, McCarthy G. Temporal cortex activation in
834 humans viewing eye and mouth movements. *Journal of neuroscience*. 1998;18(6):2188-
835 99.
- 836 28. Puce A, Allison T, McCarthy G. Electrophysiological studies of human face
837 perception. III: Effects of top-down processing on face-specific potentials. *Cerebral cortex*.
838 1999;9(5):445-58.
- 839 29. Allison T, Puce A, McCarthy G. Social perception from visual cues: role of the STS
840 region. *Trends in cognitive sciences*. 2000;4(7):267-78.
- 841 30. Hadjikhani N, Joseph RM, Snyder J, Tager-Flusberg H. Abnormal activation of the
842 social brain during face perception in autism. *Human Brain Mapping*. 2007;28(5):441-9.

- 843 31. Redcay E, Saxe R. 13 Do you see what I see? The neural bases of joint attention.
844 Agency and Joint Attention. 2013:216.
- 845 32. Harris GJ, Chabris CF, Clark J, Urban T, Aharon I, Steele S, et al. Brain activation
846 during semantic processing in autism spectrum disorders via functional magnetic
847 resonance imaging. *Brain and cognition*. 2006;61(1):54-68.
- 848 33. Lai G, Pantazatos SP, Schneider H, Hirsch J. Neural systems for speech and song
849 in autism. *Brain*. 2012;135(3):961-75.
- 850 34. Golarai G, Grill-Spector K, Reiss AL. Autism and the development of face
851 processing. *Clinical Neuroscience Research*. 2006;6(3-4):145-60.
- 852 35. Etkin A, Klemenhagen KC, Dudman JT, Rogan MT, Hen R, Kandel ER, et al.
853 Individual differences in trait anxiety predict the response of the basolateral amygdala to
854 unconsciously processed fearful faces. *Neuron*. 2004;44(6):1043-55.
- 855 36. Trevisan DA, Roberts N, Lin C, Birmingham E. How do adults and teens with self-
856 declared Autism Spectrum Disorder experience eye contact? A qualitative analysis of first-
857 hand accounts. *PLoS ONE*. 2017;12(11):e0188446.
- 858 37. Hasson U, Frith CD. Mirroring and beyond: Coupled dynamics as a generalized
859 framework for modelling social interactions. *Philosophical Transactions of the Royal
860 Society B: Biological Sciences*. 2016;371(1693):20150366.
- 861 38. Redcay E, Schilbach L. Using second-person neuroscience to elucidate the
862 mechanisms of social interaction. *Nature Reviews Neuroscience*. 2019;20(8):495-505.
- 863 39. Schilbach L, Timmermans B, Reddy V, Costall A, Bente G, Schlicht T, et al. Toward
864 a second-person neuroscience. *Behavioral and Brain Sciences*. 2013;36(04):393-414.
- 865 40. Bolis D, Schilbach L. Observing and participating in social interactions: Action
866 perception and action control across the autistic spectrum. *Dev Cogn Neuros-Neth*.
867 2018;29:168-75.
- 868 41. Rolison MJ, Naples AJ, McPartland JC. Interactive social neuroscience to study
869 autism spectrum disorder. *The Yale Journal of Biology and Medicine*. 2015;88(1):17-24.

- 870 42. Boas DA, Elwell CE, Ferrari M, Taga G. Twenty years of functional near-infrared
871 spectroscopy: introduction for the special issue. Elsevier; 2014.
- 872 43. Ferrari M, Quaresima V. A brief review on the history of human functional near-
873 infrared spectroscopy (fNIRS) development and fields of application. *Neuroimage*.
874 2012;63(2):921-35.
- 875 44. Carter RM, Huettel SA. A nexus model of the temporal-parietal junction. *Trends in*
876 *Cognitive Sciences*. 2013;17(7):328-36.
- 877 45. Hirsch J, Zhang X, Noah JA, Ono Y. Frontal temporal and parietal systems
878 synchronize within and across brains during live eye-to-eye contact. *Neuroimage*.
879 2017;157:314-30.
- 880 46. Kelley M, Noah JA, Zhang X, Scassellati B, Hirsch J. Comparison of human social
881 brain activity during eye-contact with another human and a humanoid robot. *Frontiers in*
882 *Robotics and AI*. 2021;7:599581.
- 883 47. Noah JA, Zhang X, Dravida S, Ono Y, Naples A, McPartland JC, et al. Real-time
884 eye-to-eye contact is associated with cross-brain neural coupling in angular gyrus.
885 *Frontiers in Human Neuroscience*. 2020;14:19.
- 886 48. Braddick O, Atkinson J, Wattam-Bell J. Normal and anomalous development of
887 visual motion processing: motion coherence and 'dorsal-stream vulnerability'.
888 *Neuropsychologia*. 2003;41(13):1769-84.
- 889 49. Lord C, Rutter M, DiLavore P, Risi S, Gotham K, Bishop S. Autism Diagnostic
890 Observation Schedule. Western Psychological Services. Los Angeles, CA. 2012.
- 891 50. Constantino JN, Gruber CP. Social responsiveness scale, second edition (SRS-2):
892 Manual. Los Angeles, CA: Western Psychological Services 2012.
- 893 51. Oldfield RC. The assessment and analysis of handedness: The Edinburgh
894 inventory. *Neuropsychologia*. 1971;9(1):97-113.
- 895 52. Wechsler D. WASI-II: Wechsler Abbreviated Scale of Intelligence®, Second Edition.
896 San Antonio, TX: NCS Pearson; 2011.

- 897 53. Baron-Cohen S, Wheelwright S, Skinner R, Martin J, Clubley E. The autism-
898 spectrum quotient (AQ): Evidence from asperger syndrome/high-functioning autism, males
899 and females, scientists, and mathematicians. *Journal of Autism and Developmental*
900 *Disorders*. 2001;31(1):5-17.
- 901 54. Hurley RS, Losh M, Parlier M, Reznick JS, Piven J. The broad autism phenotype
902 questionnaire. *Journal of Autism and Developmental Disorders*. 2007;37(9):1679-90.
- 903 55. Beck AT, Steer RA. Relationship between the Beck anxiety inventory and the
904 Hamilton anxiety rating scale with anxious outpatients. *Journal of Anxiety Disorders*.
905 1991;5(3):213-23.
- 906 56. Spielberger C, Gorsuch R, Lushene R. State-trait anxiety inventory (STAI). . Palo
907 Alto, CA: Mind Garden; 1983.
- 908 57. Fresco D, Coles M, Heimberg RG, Liebowitz M, Hami S, Stein MB, et al. The
909 Liebowitz Social Anxiety Scale: A comparison of the psychometric properties of self-report
910 and clinician-administered formats. *Psychological Medicine*. 2001;31(6):1025-35.
- 911 58. Champely S, Ekstrom C, Dalgaard P, Gill J, Weibelzahl S, Anandkumar A, et al.
912 pwr: Basic functions for power analysis. 2017.
- 913 59. Falck-Ytter T. Gaze performance during face-to-face communication: A live eye
914 tracking study of typical children and children with autism. *Research in Autism Spectrum*
915 *Disorders*. 2015;17:78-85.
- 916 60. Thorup E, Nyström P, Gredebäck G, Bölte S, Falck-Ytter T. Altered gaze following
917 during live interaction in infants at risk for autism: an eye tracking study. *Molecular autism*.
918 2016;7(1):1-10.
- 919 61. Dravida S, Noah JA, Zhang X, Hirsch J. Joint attention during live person-to-person
920 contact activates rTPJ, including a sub-component associated with spontaneous eye-to-
921 eye contact. *Frontiers in Human Neuroscience*. 2020;14.
- 922 62. Zhang X, Noah JA, Hirsch J. Separation of the global and local components in
923 functional near-infrared spectroscopy signals using principal component spatial filtering.
924 *Neurophotonics*. 2016;3(1):015004.

- 925 63. Noah JA, Ono Y, Nomoto Y, Shimada S, Tachibana A, Zhang X, et al. fMRI
926 validation of fNIRS measurements during a naturalistic task. *Journal of Visualized*
927 *Experiments: JoVE*. 2015(100).
- 928 64. Zhang X, Noah JA, Dravida S, Hirsch J. Signal processing of functional NIRS data
929 acquired during overt speaking. *Neurophotonics*. 2017;4(4):041409.
- 930 65. Noah JA, Dravida S, Zhang X, Yahil S, Hirsch J. Neural correlates of conflict
931 between gestures and words: A domain-specific role for a temporal-parietal complex.
932 *PLoS ONE*. 2017;12(3):e0173525.
- 933 66. Dravida S, Noah JA, Zhang X, Hirsch J. Comparison of oxyhemoglobin and
934 deoxyhemoglobin signal reliability with and without global mean removal for digit
935 manipulation motor tasks. *Neurophotonics*. 2018;5(1):011006.
- 936 67. Hirsch J, Noah JA, Zhang X, Dravida S, Ono Y. A cross-brain neural mechanism for
937 human-to-human verbal communication. *Social Cognitive and Affective Neuroscience*.
938 2018;13(9):907-20.
- 939 68. Piva M, Zhang X, Noah JA, Chang SW, Hirsch J. Distributed neural activity patterns
940 during human-to-human competition. *Frontiers in Human Neuroscience*. 2017;11:571.
- 941 69. Ono Y, Nomoto Y, Tanaka S, Sato K, Shimada S, Tachibana A, et al.
942 Frontotemporal oxyhemoglobin dynamics predict performance accuracy of dance
943 simulation gameplay: Temporal characteristics of top-down and bottom-up cortical
944 activities. *Neuroimage*. 2014;85:461-70.
- 945 70. Tachibana A, Noah JA, Bronner S, Ono Y, Onozuka M. Parietal and temporal
946 activity during a multimodal dance video game: An fNIRS study. *Neuroscience Letters*.
947 2011;503(2):125-30.
- 948 71. Okamoto M, Dan I. Automated cortical projection of head-surface locations for
949 transcranial functional brain mapping. *Neuroimage*. 2005;26(1):18-28.
- 950 72. Singh AK, Okamoto M, Dan H, Jurcak V, Dan I. Spatial registration of multichannel
951 multi-subject fNIRS data to MNI space without MRI. *Neuroimage*. 2005;27(4):842-51.

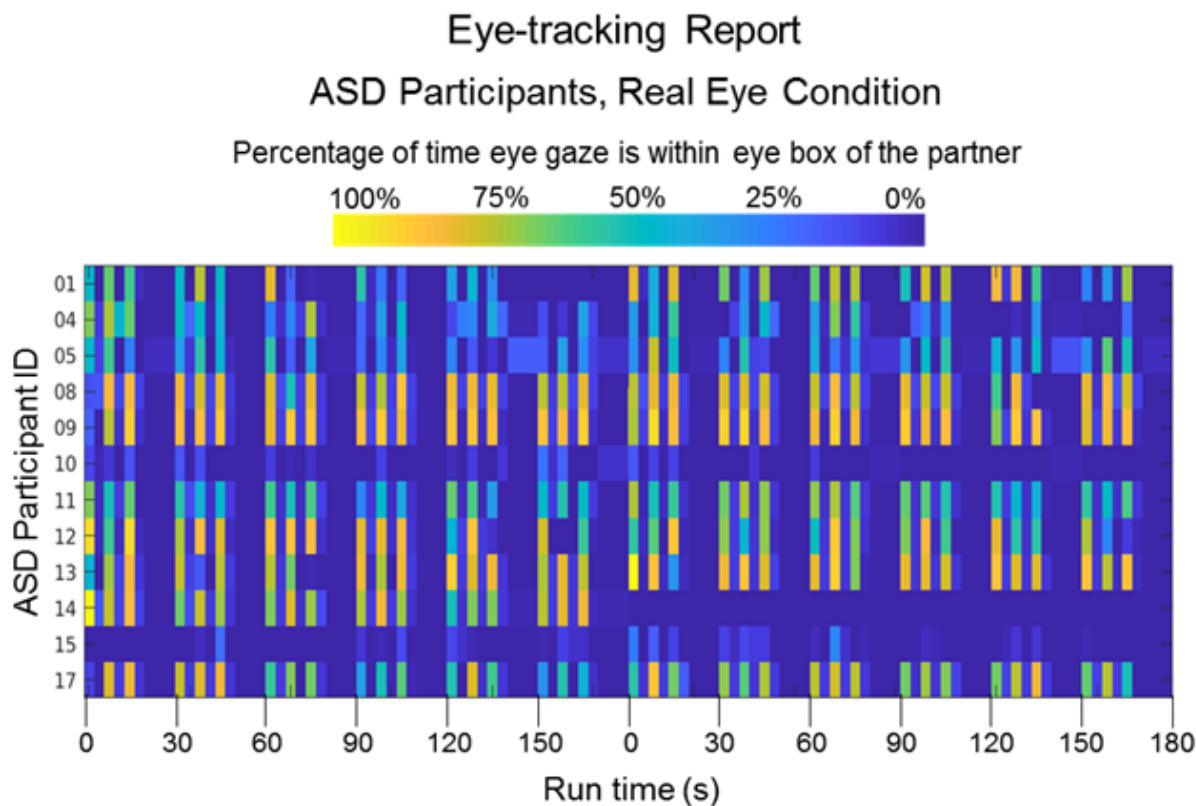
- 952 73. Eggebrecht AT, Ferradal SL, Robichaux-Viehoever A, Hassanpour MS, Dehghani
953 H, Snyder AZ, et al. Mapping distributed brain function and networks with diffuse optical
954 tomography. *Nature Photonics*. 2014;8(6):448.
- 955 74. Ferradal SL, Eggebrecht AT, Hassanpour M, Snyder AZ, Culver JP. Atlas-based
956 head modeling and spatial normalization for high-density diffuse optical tomography: In
957 vivo validation against fMRI. *Neuroimage*. 2014;85:117-26.
- 958 75. Eggebrecht AT, White BR, Ferradal SL, Chen C, Zhan Y, Snyder AZ, et al. A
959 quantitative spatial comparison of high-density diffuse optical tomography and fMRI
960 cortical mapping. *Neuroimage*. 2012;61(4):1120-8.
- 961 76. Mazziotta J, Toga A, Evans A, Fox P, Lancaster J, Zilles K, et al. A probabilistic
962 atlas and reference system for the human brain: International Consortium for Brain
963 Mapping (ICBM). *Philosophical Transactions of the Royal Society B: Biological Sciences*.
964 2001;356(1412):1293-322.
- 965 77. Ye JC, Tak S, Jang KE, Jung J, Jang J. NIRS-SPM: statistical parametric mapping
966 for near-infrared spectroscopy. *Neuroimage*. 2009;44(2):428-47.
- 967 78. Maldjian JA, Laurienti PJ, Kraft RA, Burdette JH. An automated method for
968 neuroanatomic and cytoarchitectonic atlas-based interrogation of fMRI data sets.
969 *Neuroimage*. 2003;19(3):1233-9.
- 970 79. Maldjian JA, Laurienti PJ, Burdette JH. Precentral gyrus discrepancy in electronic
971 versions of the Talairach atlas. *Neuroimage*. 2004;21(1):450-5.
- 972 80. Hazeki O, Tamura M. Quantitative analysis of hemoglobin oxygenation state of rat
973 brain in situ by near-infrared spectrophotometry. *Journal of Applied Physiology*.
974 1988;64(2):796-802.
- 975 81. Hoshi Y. Functional near-infrared optical imaging: Utility and limitations in human
976 brain mapping. *Psychophysiology*. 2003;40(4):511-20.
- 977 82. Matcher SJ, Elwell CE, Cooper CE, Cope M, Delpy DT. Performance comparison of
978 several published tissue near-infrared spectroscopy algorithms. *Anal Biochem*.
979 1995;227(1):54-68.

- 980 83. Yücel M, Lühmann A, Scholkmann F, Gervain J, Dan I, Ayaz H, et al. Best practices
981 for fNIRS publications. *Neurophotonics*. 2021;8(1):012101.
- 982 84. Tachtsidis I, Scholkmann F. False positives and false negatives in functional near-
983 infrared spectroscopy: Issues, challenges, and the way forward. *Neurophotonics*.
984 2016;3(3):031405.
- 985 85. Noah JA, Zhang X, Dravida S, DiCocco C, Suzuki T, Aslin RN, et al. Comparison of
986 short-channel separation and spatial domain filtering for removal of non-neural
987 components in functional near-infrared spectroscopy signals. *Neurophotonics*.
988 2021;8(1):015004.
- 989 86. Tachtsidis I, Tisdall MM, Leung TS, Pritchard C, Cooper CE, Smith M, et al.
990 Relationship between brain tissue haemodynamics, oxygenation and metabolism in the
991 healthy human adult brain during hyperoxia and hypercapnea. *Oxygen Transport to*
992 *Tissue XXX*: Springer; 2009. p. 315-20.
- 993 87. Penny WD, Friston KJ, Ashburner JT, Kiebel SJ, Nichols TE. *Statistical parametric*
994 *mapping: The analysis of functional brain images*: Elsevier; 2011.
- 995 88. de Vries L, Fouquaet I, Boets B, Naulaers G, Steyaert J. Autism spectrum disorder
996 and pupillometry: A systematic review and meta-analysis. *Neuroscience & Biobehavioral*
997 *Reviews*. 2021;120:479-508.
- 998 89. Schroeder CE, Wilson DA, Radman T, Scharfman H, Lakatos P. Dynamics of active
999 sensing and perceptual selection. *Current Opinion in Neurobiology*. 2010;20(2):172-6.
- 1000 90. Zweifel NO, Hartmann MJ. Defining “active sensing” through an analysis of sensing
1001 energetics: Homeoactive and alloactive sensing. *Journal of Neurophysiology*.
1002 2020;124(1):40-8.
- 1003 91. Simmons DR, Robertson AE, McKay LS, Toal E, McAleer P, Pollick FE. Vision in
1004 autism spectrum disorders. *Vision Research*. 2009;49(22):2705-39.
- 1005 92. Goldberg M, Lasker A, Zee D, Garth E, Tien A, Landa R. Deficits in the initiation of
1006 eye movements in the absence of a visual target in adolescents with high functioning
1007 autism. *Neuropsychologia*. 2002;40(12):2039-49.

- 1008 93. Haxby JV, Hoffman EA, Gobbini MI. The distributed human neural system for face
1009 perception. *Trends in Cognitive Sciences*. 2000;4(6):223-33.
- 1010 94. Kanwisher N, McDermott J, Chun MM. The fusiform face area: A module in human
1011 extrastriate cortex specialized for face perception. *Journal of Neuroscience*.
1012 1997;17(11):4302-11.
- 1013 95. Chang L, Tsao DY. The code for facial identity in the primate brain. *Cell*.
1014 2017;169(6):1013-28. e14.
- 1015 96. Johnson MH, Griffin R, Csibra G, Halit H, Farroni T, de Haan M, et al. The
1016 emergence of the social brain network: Evidence from typical and atypical development.
1017 *Development and Psychopathology*. 2005;17(03):599-619.
- 1018 97. Scholkmann F, Holper L, Wolf U, Wolf M. A new methodical approach in
1019 neuroscience: Assessing inter-personal brain coupling using functional near-infrared
1020 imaging (fNIRI) hyperscanning. *Frontiers in Human Neuroscience*. 2013;7:813.
- 1021 98. Babiloni F, Astolfi L. Social neuroscience and hyperscanning techniques: Past,
1022 present and future. *Neuroscience & Biobehavioral Reviews*. 2014;44:76-93.
- 1023 99. Bilek E, Ruf M, Schäfer A, Akdeniz C, Calhoun VD, Schmahl C, et al. Information
1024 flow between interacting human brains: Identification, validation, and relationship to social
1025 expertise. *Proceedings of the National Academy of Sciences*. 2015;112(16):5207-12.
- 1026 100. Wheatley T, Boncz A, Toni I, Stolk A. Beyond the isolated brain: the promise and
1027 challenge of interacting minds. *Neuron*. 2019;103(2):186-8.
- 1028 101. Kingsbury L, Hong W. A multi-brain framework for social interaction. *Trends in*
1029 *Neurosciences*. 2020;43(9):651-66.
- 1030 102. Hasson U, Ghazanfar AA, Galantucci B, Garrod S, Keysers C. Brain-to-brain
1031 coupling: A mechanism for creating and sharing a social world. *Trends in Cognitive*
1032 *Sciences*. 2012;16(2):114-21.

- 1033 103. De Jaegher H, Di Paolo E, Adolphs R. What does the interactive brain hypothesis
1034 mean for social neuroscience? A dialogue. *Philosophical Transactions of the Royal Society*
1035 *B: Biological Sciences*. 2016;371(1693):20150379.
- 1036 104. Di Paolo EA, De Jaegher H. The interactive brain hypothesis. *Frontiers in Human*
1037 *Neuroscience*. 2012;6.
- 1038 105. Redcay E, Kleiner M, Saxe R. Look at this: The neural correlates of initiating and
1039 responding to bids for joint attention. *Frontiers in Human Neuroscience*. 2012;6:169.
- 1040 106. Huppert TJ, Hoge RD, Diamond SG, Franceschini MA, Boas DA. A temporal
1041 comparison of BOLD, ASL, and NIRS hemodynamic responses to motor stimuli in adult
1042 humans. *Neuroimage*. 2006;29(2):368-82.
- 1043 107. Jöbsis FF. Noninvasive, infrared monitoring of cerebral and myocardial oxygen
1044 sufficiency and circulatory parameters. *Science*. 1977;198(4323):1264-7.
- 1045 108. Strangman G, Culver JP, Thompson JH, Boas DA. A quantitative comparison of
1046 simultaneous BOLD fMRI and NIRS recordings during functional brain activation.
1047 *Neuroimage*. 2002;17(2):719-31.
- 1048 109. Villringer A, Chance B. Non-invasive optical spectroscopy and imaging of human
1049 brain function. *Trends in Neurosciences*. 1997;20(10):435-42.
- 1050 110. Scherf KS, Elbich D, Minshew N, Behrmann M. Individual differences in symptom
1051 severity and behavior predict neural activation during face processing in adolescents with
1052 autism. *NeuroImage: Clinical*. 2015;7:53-67.
- 1053 111. McPartland JC. Developing clinically practicable biomarkers for autism spectrum
1054 disorder. *Journal of autism and developmental disorders*. 2017;47(9):2935-7.
- 1055 112. Chan AW, Downing PE. Faces and eyes in human lateral prefrontal cortex.
1056 *Frontiers in human neuroscience*. 2011;5:51.
- 1057 113. Happé F, Frith U. The weak coherence account: detail-focused cognitive style in
1058 autism spectrum disorders. *Journal of autism and developmental disorders*. 2006;36(1):5-
1059 25.

1060 **Supporting Information**



1061

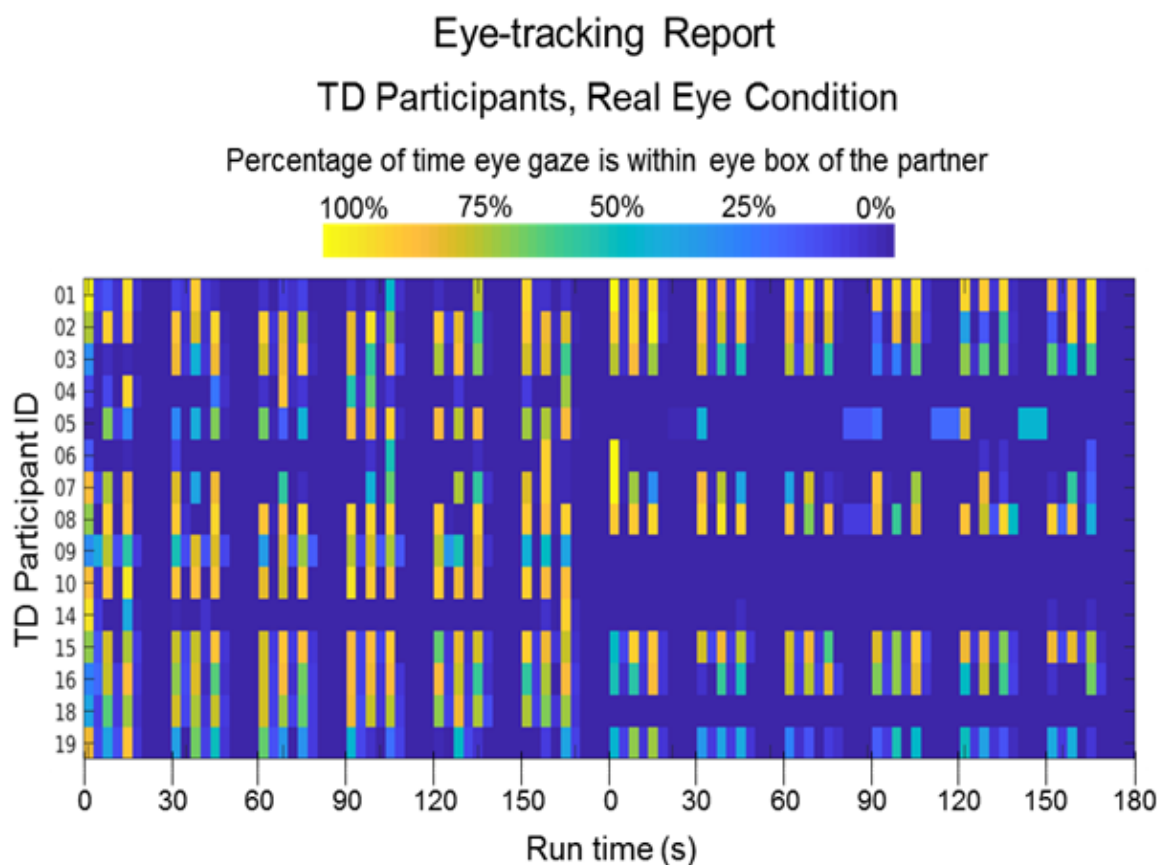
1062

S1 Fig. Eye tracking Report for Autism Spectrum Disorder (ASD) Participants, Real Eye Condition. Colors indicate the percentage of time eye gaze is within the eye region of the partner (dark blue = 0% and bright yellow = 100%) during each epoch of the time series (x-axis). The vertical axis includes all ASD participants for whom eye tracking data were acquired.

1063

1064

1065



1066

S2 Fig. Eye tracking Report for Typically-Developed (TD) Participants, Real Eye Condition. Colors indicate the percentage of time eye gaze is within the eye region of the partner (dark blue = 0% and bright yellow = 100%) during each epoch of the time series (x-axis). The vertical axis includes all TD participants for whom eye tracking data were acquired.

1067

Study Participants and Behavioral Test Scores: ASD

| ID | M/F | Age | FSIQ-4 | AQ | BAPQ | SRS-2 | BAI | STAI | LSAS | ADOS-2 | Eye tracking |
|----|--------|-------|--------|----|------|-------|-----|------|------|--------|--------------|
| 1 | Male | 28-32 | 114 | 26 | 123 | 54 | 16 | 21 | 30 | 12 | Yes |
| 2 | Male | 33-37 | 104 | 23 | 121 | 30 | 8 | 31 | 0 | 15 | * |
| 3 | Male | 28-32 | 112 | 30 | 137 | 82 | 11 | 27 | 46 | 16 | * |
| 4 | Male | 23-27 | 108 | 15 | 102 | 53 | 21 | 30 | 56 | 14 | Yes |
| 5 | Male | 23-27 | 97 | 15 | 99 | 41 | 19 | 29 | 43 | 10 | Yes |
| 6 | Male | 23-27 | 90 | 26 | 131 | 132 | 41 | 53 | 79 | 16 | * |
| 7 | Male | 28-32 | 113 | 15 | 94 | 68 | 7 | 44 | 44 | 13 | * |
| 8 | Male | 18-22 | 95 | 24 | 117 | 79 | 24 | 37 | 38 | 15 | Yes |
| 9 | Male | 18-22 | 101 | 30 | 140 | 96 | 27 | 46 | 85 | 18 | Yes |
| 10 | Female | 28-32 | 110 | 20 | 124 | 70 | 9 | 61 | 34 | 17 | Yes |
| 11 | Female | 18-22 | 128 | 32 | 121 | 68 | 4 | 30 | 32 | 9 | Yes |
| 12 | Male | 18-22 | 124 | 25 | 128 | 60 | 1 | 35 | 44 | 9 | Yes |
| 13 | Male | 18-22 | 107 | 14 | 95 | 34 | 9 | 55 | 5 | 12 | Yes |
| 14 | Male | 18-22 | 121 | 30 | 155 | 103 | 17 | 41 | 77 | 11 | Yes |
| 15 | Male | 23-27 | 112 | 20 | 117 | 36 | 3 | 23 | 3 | 13 | Yes |
| 16 | Male | 28-32 | 101 | 47 | 189 | 153 | 25 | 67 | 126 | 12 | * |
| 17 | Female | 28-32 | 109 | 23 | 94 | 65 | 15 | 33 | 38 | 11 | Yes |

*Data unavailable

1068

1069 **S1 Table.** Demographic information for Autism Spectrum Disorder (ASD) participants.
 1070 Assessment measures include the Autism-Spectrum Quotient test (AQ, total scores); Broad
 1071 Autism Phenotype Questionnaire (BAPQ, total scores); Social Responsiveness Scale, Second
 1072 Edition (SRS-2, raw scores); Beck Anxiety Inventory (BAI, total scores); State-Trait Anxiety
 1073 Inventory (STAI; total state anxiety scores); Liebowitz Social Anxiety Scale (LSAS, total scores);
 1074 and the Autism Diagnostic Observation Schedule (ADOS-2, total scores). The Wechsler
 1075 Abbreviated Scale of Intelligence, 2nd Edition (WASI-II) was administered to estimate full-scale
 1076 intelligence quotient scores based on four subtests (FSIQ-4). *Indicates data are unavailable.

1077

Study Participants and Behavioral Test Scores: TD

| ID | M/F | Age | FSIQ-4 | AQ | BAPQ | SRS-2 | BAI | STAI | LSAS | Eye tracking |
|----|--------|-------|--------|----|------|-------|-----|------|------|--------------|
| 1 | Male | 18-22 | * | 12 | 77 | 52 | 10 | * | 23 | Yes |
| 2 | Male | 18-22 | 123 | 23 | 118 | 55 | 4 | 39 | 52 | Yes |
| 3 | Male | 28-32 | 113 | 6 | 85 | 9 | 4 | 26 | 24 | Yes |
| 4 | Male | 23-27 | * | * | 72 | 16 | * | * | * | Yes |
| 5 | Female | 23-27 | 129 | 6 | 70 | 20 | 1 | 25 | 23 | Yes |
| 6 | Female | 23-27 | 114 | 8 | 79 | 27 | 5 | 28 | 43 | Yes |
| 7 | Female | 28-32 | 103 | 1 | 53 | 6 | 3 | 21 | 22 | Yes |
| 8 | Male | 28-32 | * | 26 | 109 | 48 | 0 | 23 | 23 | Yes |
| 9 | Female | 18-22 | 79 | 32 | 121 | 64 | 5 | 37 | 44 | Yes |
| 10 | Female | 23-27 | 119 | 22 | 111 | 37 | 26 | 62 | 60 | Yes |
| 11 | Female | 28-32 | 107 | 14 | 88 | 36 | 2 | 29 | 63 | * |
| 12 | Male | 28-32 | 111 | 10 | 73 | 25 | 5 | 28 | 27 | * |
| 13 | Female | 23-27 | 126 | 14 | 93 | 43 | 10 | 38 | 12 | * |
| 14 | Male | 18-22 | * | 25 | 105 | 84 | 7 | 27 | 59 | Yes |
| 15 | Female | 23-27 | 122 | 7 | 79 | 12 | 0 | 26 | 32 | Yes |
| 16 | Male | 38-42 | * | 21 | 124 | 63 | 9 | 56 | 56 | Yes |
| 17 | Male | 18-22 | * | 19 | 96 | 45 | 0 | 22 | 45 | * |
| 18 | Male | 28-32 | 119 | 19 | 89 | 38 | 12 | 26 | 46 | Yes |
| 19 | Male | 38-42 | 121 | 10 | 73 | 31 | 0 | 20 | 18 | Yes |

*Data unavailable

1078

1079 **S2 Table.** Demographic information for Typically-Developed (TD) participants. Assessment
 1080 measures include the Autism-Spectrum Quotient test (AQ, total scores); Broad Autism
 1081 Phenotype Questionnaire (BAPQ, total scores); Social Responsiveness Scale, Second Edition
 1082 (SRS-2, raw scores); Beck Anxiety Inventory (BAI, total scores); State-Trait Anxiety Inventory
 1083 (STAI; total state anxiety scores); and the Liebowitz Social Anxiety Scale (LSAS, total scores).
 1084 The Wechsler Abbreviated Scale of Intelligence, 2nd Edition (WASI-II) was administered to
 1085 estimate full-scale intelligence quotient scores based on four subtests (FSIQ-4). *Indicates data
 1086 are unavailable.

1087

Comparison of ASD and TD Groups by Gender, Handedness, and Age

| | ASD | TD | n | % |
|--------------------|-------|-------|-----------|-------|
| Female | 3 | 8 | 11 | 31% |
| Male | 14 | 11 | 25 | 69% |
| n | 17 | 19 | 36 | |
| % | 47% | 53% | | |
| Handedness | | | | |
| Right | 12 | 18 | 30 | 83.3% |
| Left | 3 | 0 | 3 | 8.3% |
| Ambidextrous | 2 | 1 | 3 | 8.3% |
| Age (years) | | | | |
| Mean | 25 | 26 | | |
| Median | 26 | 26 | | |
| Range | 18-34 | 19-38 | | |
| SD | ± 4.9 | ± 5.8 | | |

1088

1089 **S3 Table.** Comparison of Autism Spectrum Disorder (ASD) and Typically-Developed (TD) participant
 1090 groups by gender, handedness, and age. Groups were similar in terms of age and handedness;
 1091 however, the ratio of male to female participants was higher in the ASD group than in the TD group.
 1092 The gender composition of the ASD group is consistent with the estimated 4:1 male:female ratio of
 1093 ASD diagnosis. This ratio increases to 6 males diagnosed with ASD for every 1 female in people
 1094 whose cognitive functioning is within or above normal limits, such as those in our sample (Kirkovski,
 1095 M., Enticott, P. G., & Fitzgerald, P. B. (2013). A review of the role of female gender in autism
 1096 spectrum disorders. *Journal of Autism and Developmental Disorders*, 43(11), 2584-2603).

1097

1098

1099
1100
1101
1102
1103
1104
1105
1106
1107
1108
1109
1110
1111
1112
1113
1114
1115
1116
1117
1118
1119
1120
1121

**Statistical Comparisons of
Clinical and Behavioral Assessments
for ASD and TD Groups**

| Measure | p-value |
|---|--------------|
| Autism-Spectrum Quotient | 0.002 |
| Broad Autism Phenotype Questionnaire | 0.002 |
| Social Responsiveness Scale | 0.002 |
| Beck Anxiety Inventory | 0.016 |
| State-Trait Anxiety Inventory | 0.067 |
| Liebowitz Social Anxiety Scale | 0.363 |
| Wechsler Abbreviated Scale of Intelligence (FSIQ-4) | 0.539 |

S4 Table. Statistical comparisons (independent t-tests, two-tailed assuming unequal variances) of scores between Typically-Developed (TD) and Autism Spectrum Disorder (ASD) groups are consistent with differences for the Autism-Spectrum Quotient test; Broad Autism Phenotype Questionnaire; Social Responsiveness Scale, 2nd Edition; and the Beck Anxiety Inventory. No evidence was found for differences between the groups for FSIQ-4 (estimated by the Wechsler Abbreviated Scale of Intelligence); State-Trait Anxiety Inventory (state anxiety items only); or the Liebowitz Social Anxiety Scale, and is taken as evidence in favor of matched groups with respect to these metrics.

1122
1123
1124
1125
1126
1127
1128
1129
1130
1131
1132
1133
1134
1135
1136
1137
1138
1139
1140
1141
1142
1143
1144
1145
1146
1147
1148
1149
1150
1151

Dwell time represented as a percentage of
time eye gaze is within eye box of partner:

Group averages and individual medians

| TD | | ASD | |
|--------------------------|----------|--------------------------|----------|
| ID | Median % | ID | Median % |
| 1 | 62 | 1 | 48 |
| 2 | 75 | 4 | 33 |
| 3 | 61 | 5 | 37 |
| 4 | 24 | 8 | 71 |
| 5 | 33 | 9 | 80 |
| 6 | 9 | 10 | 5 |
| 7 | 49 | 11 | 53 |
| 8 | 78 | 12 | 63 |
| 9 | 59 | 13 | 71 |
| 10 | 85 | 14 | 69 |
| 14 | 9 | 15 | 6 |
| 15 | 77 | 17 | 62 |
| 16 | 62 | mean: 49.8 ± 25.0 | |
| 18 | 68 | | |
| 19 | 37 | | |
| mean: 52.5 ± 24.8 | | | |

S5 Table. Group averages and individual median percentages of eye-gaze time within the eye box of partners for typically developed (TD) participants (left column) and autism spectrum disorder (ASD) participants (right column) during the Real Eye Condition. A t-test of these median percentages shows $t(25) = 0.28$ n.s. See S1 and S2 Figs for a graphical run-by-run representation of eye tracking performance.